FEBS 28636 FEBS Letters 571 (2004) 187–191

# Feeding induces expression of heat shock proteins that reduce oxidative stress

Kensaku Katsuki[a,b], Mitsuaki Fujimoto[a], Xiu-Ying Zhang[a], Hanae Izu[a], Eiichi Takaki[a], Yukio Tanizawa[b], Sachiye Inouye[a], Akira Nakai[a,*]

[a]*Department of Biochemistry and Molecular Biology, Yamaguchi University School of Medicine, Minami-Kogushi 1-1-1, Ube 775-8505, Japan*
[b]*Third Department of Internal medicine, Yamaguchi University School of Medicine, Minami-Kogushi 1-1-1, Ube 775-8505, Japan*

Received 8 June 2004; revised 22 June 2004; accepted 22 June 2004

Available online 14 July 2004

Edited by Barry Halliwell

**Abstract Heat shock proteins (Hsps) are induced in response to various kinds of environmental and physiological stresses. However, it is unclear whether Hsps play roles in protecting cells in the digestive organs against xenobiotic chemicals. Here, we found that feeding induces expression of a set of Hsps specifically in the mouse liver and intestine by activating heat shock transcription factor 1 (HSF1). In the liver, HSF1 is required to suppress toxic effects of electrophiles, which are xenobiotic chemicals causing oxidative stress. We found that overexpression of Hsp27, which elevates cellular glutathione level, promotes survival of culture cells exposed to electrophiles. These results suggest a novel mechanism of cell protection against xenobiotic chemicals in the food.**


*Keywords:* Electrophile; Glutathione; Heat shock protein; Heat shock transcription factor; Liver; Oxidative stress

## 1. Introduction

Heat shock response, which is characterized by the induction of a set of heat shock proteins (Hsps), is a fundamental response in all organisms to protect themselves from environmental stresses such as heat, oxidative stress, ischemia, inflamation and exposure to toxic chemicals [1]. This response is regulated mainly at a transcription level by heat shock transcription factor 1 (HSF1) in mammals [2]. There are many Hsps belonging to diverse families and Hsps act coordinately to assist the folding of cellular proteins [3]. Hsps also bind to denatured proteins, prevent misaggregation and facilitate renaturation. In addition to the "foldase activity", each Hsp has a unique role. For example, Hsp27 reduces oxidative stress by raising the pool of reduced glutathione (GSH) in the cells [4].

In addition to environmental stresses, heat shock response is induced in response to physiological stresses such as exercise [5,6] and restraint stress [7,8]. Here, we found that feeding induces expression of Hsps selectively in the liver and intestine among digestive organs. Digested elements such as oligosaccharides, proteins, lipids and nucleic acids are adsorbed mostly in the intestine, and blood containing these elements is directly transported to the liver through the portal vein. To protect themselves from xenobiotic chemicals such as electrophiles in the food, detoxifying enzymes are rich in the liver [9,10]. We found that electrophiles induce heat shock response in HeLa and Jurkat cells, probably by causing oxidative stress. Furthermore, induction of at least Hsp27 reduced toxic effects of electrophiles on culture cells.

## 2. Materials and methods

### 2.1. Animals, food and injection of DEM

Mice of ICR background were maintained at 24 °C with light on from 8 to 20 h. 6-week-old mice had free access to water and diet (bleeding grade F-1, Oriental Yeast Co., Ltd, Tokyo, Japan). Food deprivation was performed for 48 h and then the same diet was fed for indicated periods. Digestive organs were immediately dissected and stored at −80 °C until use. To examine the expression of Hsps in the absence of HSF1, HSF1-null mice were used [11]. Diethyl maleate (DEM) (Wako, Osaka, Japan) prepared in sesame oil (5.3 mmol of DEM/kg of body weight) was injected intraperitoneally and serum alanine aminotransferase (ALT) levels were measured (SRL Co., Tokyo, Japan). All experimental protocols were reviewed by the Committee for Ethics on Animal Experiments of Yamaguchi University School of Medicine.

### 2.2. Western blot analysis, Gel shift assay and Northern blot analysis

Tissues were dissected, immediately frozen and stored at −80 °C until use. The extracts were prepared with NP-40 lysis buffer [150 mM NaCl, 1.0% Nonidet P-40, 50 mM Tris (pH 8.0), 1 mM phenylmethylsulfonyl fluoride, 1 μg/ml leupeptin and 1 μg/ml pepstatin]. HeLa cell extracts were also prepared with NP-40 lysis buffer. Western blot analysis was performed as described previously [12] using mouse monoclonal IgG for Hsp70 (W27, Santa Cruiz), and antiserum for human Hsp70 (Fujimoto, unpublished), rat Hsp27 (a kind gift from K. Kato), and human GST-pi (Novocastra Lab. Ltd., UK). To detect Hsp90, we generated a specific antiserum. Recombinant human Hsp90α (amino acids 333–732) fused to glutathione-*S*-transferase was immunized in rabbits in a TiterMax (CrtRx Co., Georgia) water-in-oil emulsion. The levels of Hsp70 protein in various tissues were estimated by using NIH image.

To perform gel shift assay, mice were systematically anesthetized with ketamine (16 mg/kg, i.p.) and xylazine (16 mg/kg, i.p.) and perfused with phosphate-buffered saline. Whole tissue extracts were prepared from the liver, and gel shift assay and supershift experiments were performed as described previously [12].

Northern blot analysis was performed essentially as described previously [13].

### 2.3. Cells and the treatment with reagents

HeLa cells were maintained at 37 °C in 5% $CO_2$ in Dulbecco's modified Eagle's medium containing 10% fetal calf serum at 37 °C in

* Corresponding author. Fax: +81-836-22-2315.
*E-mail address:* anakai@yamaguchi-u.ac.jp (A. Nakai).

0014-5793/$22.00 © 2004 Published by Elsevier B.V. on behalf of the Federation of European Biochemical Societies.
doi:10.1016/j.febslet.2004.06.087

5% $CO_2$. HeLa cells stably expressing mouse Hsp27 were described previously [14]. To prepare HeLa cells expressing human GST-pi (pcDNA3.1/GST-pi), GST-pi cDNA [15] was cloned by RT-PCR and was inserted into pcDNA3.1(+) (Invitrogen). The DNA was transfected into HeLa cells by a calcium-phosphate method and cells grown in the presence of 1.5 mg/ml of G418 were selected as described previously [14]. Jurkat cells were maintained in RPMI containing 10% fetal calf serum. To block de novo synthesis of glutathione, cells were treated with 0.1 mM L-buthionine-(*S,R*)-sulfoximine (BSO) (stock, 100 mM in $H_2O$) (Sigma, St. Louis, MO) until 48 h. Cells were also treated with electrophile, 1-chloro-2,4-dinitrobenzene (CDNB) (stock, 10 mM in 100% ethanol) or DEM (stock, 10 mM in 100% ethanol) at a concentration of 10 to 40 μM for 8 h.

To examine cell survival, HeLa cells were treated with CDNB for 24 h and were replated in dishes containing normal medium for 10 days. Cells were fixed in 70% ethanol for 30 min and then stained with Giemsa's stain solution (Muto Pure Chemicals, Tokyo, Japan). Colonies counted, and means and S.D. were calculated from three independent experiments.

*2.4. Determination of glutathione levels*

Total cellular glutathione concentrations (reduced plus oxidized forms) were measured as described previously [16,17] and showed as nanomoles per $1 \times 10^6$ cells.

## 3. Results

*3.1. Feeding induces heat shock response specifically in the liver and intestine*

To reveal whether feeding induces expression of Hsps in various tissues, mice starved for 48 h were fed for 3 h and expression of Hsp70 protein was determined. We found that Hsp70 expression was induced in the liver and the intestine after feeding, but was not induced in the colon, stomach, brain and muscle (Fig. 1A). As the liver is important for detoxifying chemicals, we further analyzed the response in the liver. Inductions of proteins and mRNAs of Hsp70 and Hsp90 were observed even 1 h after feeding, and induction of Hsp27 protein was particularly strong although it was detected firstly at 6 h after feeding (Fig. 1B). Induction of Hsp70 was low probably due to unique regulation of Hsp70 in the liver [18].

*3.2. HSF1 plays roles in suppressing toxic effects of electrophiles in the liver*

We next examined HSF1 activation in the liver. Weak, but distinct HSE-binding activity of HSF was induced 1 h after feeding in the liver and then the activity attenuated (Fig. 2A). Supershift experiment using specific antiserum showed that the HSE-binding activity was composed of HSF1 (data not shown). We next examined the induction of Hsp90, Hsp70 and Hsp27 expression after feeding in HSF1-null mice. We observed no induction of Hsps in HSF1-null mice (Fig. 2B), indicating that HSF1 is required for the feeding-induced induction of Hsps in the liver.

To examine whether HSF1 plays roles in rendering toxic effects of xenobiotic chemicals in the liver, an electrophilic reagent DEM was injected intraperitoneally. We determined toxic effects of DEM on liver cells by estimating levels of serum ALT that is released from damaged liver cells. We found that serum ALT levels did not increase in both wild-type starved and feeding mice injected with 5.3 mmol of DEM/kg of body weight (41.7 and 30.7 IU/L, respectively), but increased in DEM-injected starved HSF1-null mice (69.7 IU/L) (Fig. 2C). Furthermore, ALT level in DEM-injected feeding HSF1-null mice (174.3 IU/L) was much higher than that in starved mice.

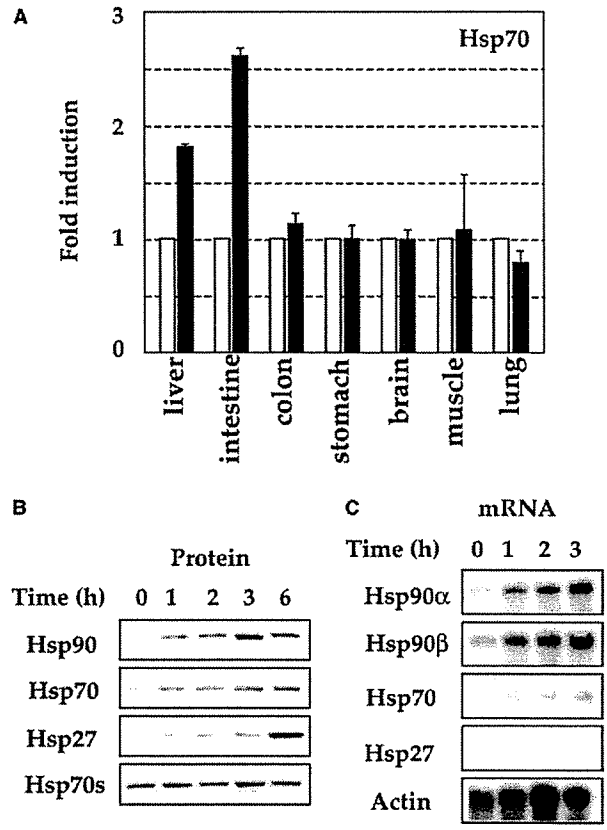


Fig. 1. Feeding induces heat shock response in the liver and intestine. (A) 6-week-old mice were starved for 48 h (open bars) and then fed for 3 h (closed bars). Expression levels of Hsp70 in various tissues were determined by Western blot analysis and were normalized by expression levels of β-actin. Means and S.D. of fold inductions from three independent experiments are shown. (B) Starved mice for 48 h (0) were fed for 1, 2, 3 and 6 h. Expression levels of Hsps in the liver were determined by Western blot analysis using each specific antibody and antibody recognizing Hsp70 and Hsc70 (Hsp70s). Representative data are shown from three experiments. (C) Starved mice for 48 h (0) were fed for 1, 2 and 3 h. Expression levels of Hsps in the liver were determined by Northern blot analysis using each specific cDNA probes. Representative data are shown from three experiments.

These results suggest that HSF1 plays roles in suppressing toxic effects of electrophiles in the liver.

*3.3. Electrophiles induce heat shock response*

As we found a little induction of Hsps in the liver by injection with 5.3 mmol of DEM/kg of body weight (data not shown), we analyzed the response of cultured HeLa and Jurkat cells to electrophiles. We found that electrophiles, both DEM and CDNB, induced activation of HSF1 and expression of Hsp70 (Fig. 3A and B, data not shown). BSO reduces de novo synthesis of cellular glutathione level (Fig. 3C), and Hsp90, Hsp70, Hsp40 and Hsp27 were induced at lower concentrations of CDNB when the level of glutathione was reduced (Fig. 3D). These results suggest that electrophiles cause oxidative stress that induces heat shock response.

*3.4. Hsp27 reduces toxic effects of electrophiles on culture cells*

Because Hsp27 expression is markedly induced by the feeding and was too low to be detected in HSF1-null liver

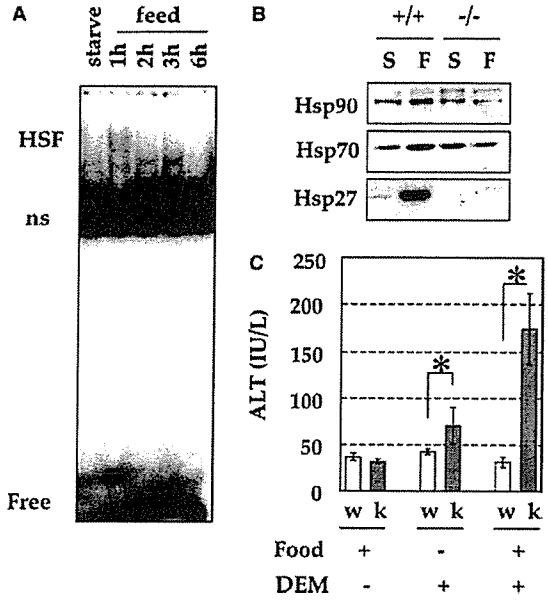


Fig. 2. HSF1 is required for feeding-induced induction of Hsps and protection from an electrophile in the liver. (A) Starved mice for 48 h (starvation) were fed for 1, 2, 3 and 6 h. HSE-binding activities in the liver extracts were determined by gel shift assay using a $^{32}$P-labelled HSE-oligonucleotide. HSF, complexes of HSF and HSE-probe; Free, free oligonucleotide; ns, non-specific binding. (B) 6-week-old wild-type (+/+) and HSF1-null (−/−) mice were starved for 48 h (S), and then fed for 6 h (F). Expression levels of Hsp90, Hsp70 and Hsp27 were determined by Western blot analysis. (C) In a starved mouse group (food −), wild-type (w) and HSF1-null (k) mice were starved for 42 h and were injected with DEM. At 6 h after the injection, mice were fed for 24 h and serum ALT levels were determined. In a fed mouse group (food +), mice were starved for 42 h. After they were fed for 6 h, mice were injected with DEM. Serum ALT levels were determined 24 h after the injection. Serum ATL levels were also determined without DEM injection (DEM −). Means and S.D. from three experiments are shown. Stars indicate $P < 0.05$. Representative data are shown from at least three experiments.

(Fig. 2B), we examined whether overexpression of Hsp27 into HeLa cells [14] reduces toxic effects caused by electrophiles. As a control, we also generate HeLa cells overexpressing GST-pi (GST/HeLa), which promotes conjugation of glutathione to chemicals. Glutathione level was increased twofold in Hsp27/HeLa cells. Induction of Hsp70 was observed in response to 40 μM of CDNB in HeLa and GST/HeLa cells, whereas we detect no induction of Hsp70 in Hsp27/HeLa cells even in the presence of 40 μM of CDNB. Overexpression of Hsp27 prevented the induction of HSE-binding activity (data not shown). Furthermore, we found that survival of cells exposed to CDNB was significantly promoted in the presence of Hsp27 (Fig. 4D). These results indicate that induction of Hsp27 reduces toxic effects of electrophiles on culture cells.

## 4. Discussion

Digestive organs are frequently exposed to xenobiotic chemicals in food. These chemicals are adsorbed in the small intestine and then transported into the liver, where xenobiotic chemicals are mainly detoxified [9,10]. Therefore, it is interesting to show that feeding induces the heat shock response only in the liver and small intestine among digestive organs. Previously, it was reported that feeding induces molecular chaperones located in the endoplasmic reticulum in the liver [19,20]. However, this is the first demonstration that feeding induces a set of cytoplasmic Hsps. Furthermore, we found that feeding induces heat shock response by activating HSF1, which is also activated by heat shock [2]. Although heat shock-induced activation of HSF1 is triggered by denaturation of cellular proteins, it is unlikely that normal food induces denaturation of proteins. HSF1 may be activated through an unknown pathway to cope with unexpected toxicants such as electrophilic agents in the food.

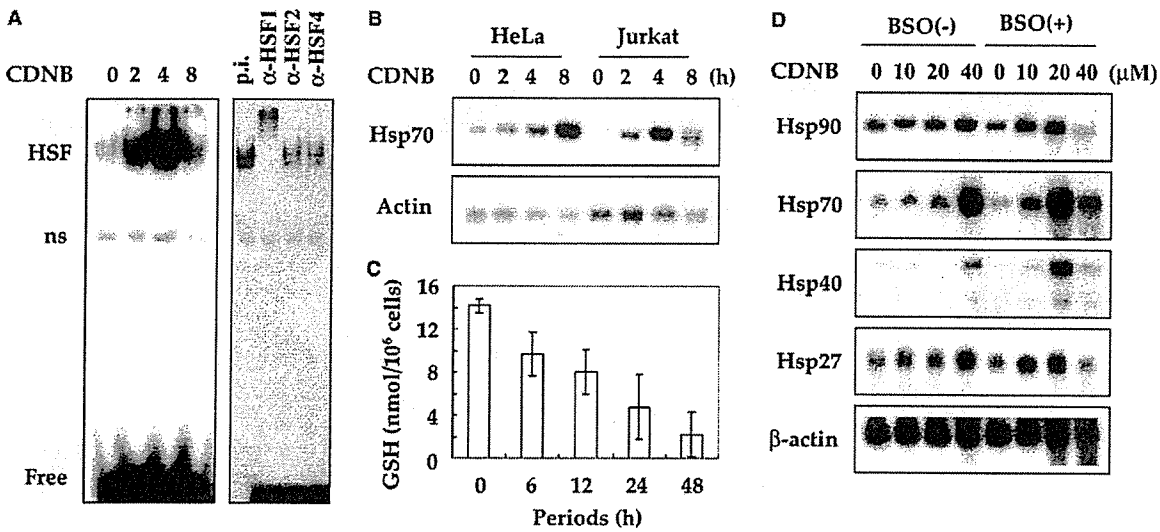


Fig. 3. CDNB induces heat shock response. (A) HeLa cells were treated with 40 μM of CDNB for indicated periods and gel shift assay was performed using a $^{32}$P-labelled HSE-oligonucleotide (left). A supershift experiment of extract prepared from cells treated with CDNB for 4 h using preimmune serum (p.i.) or each specific antiserum. (B) HeLa and Jurkat cells were treated with CDNB as described in A. Northern blot analysis was performed using a cDNA probe specific for Hsp70 or β-actin. (C) HeLa cells were treated with 0.1 mM BSO for indicated periods. Levels of GSH were measured. Means and S.D. of three independent experiments are shown. (D) HeLa cells were treated with 0.1 mM BSO for 40 h and further incubated in the presence of 0, 10, 20 or 40 mM CDNB for 8 h. Total RNAs were isolated and Northern blot analysis was performed.

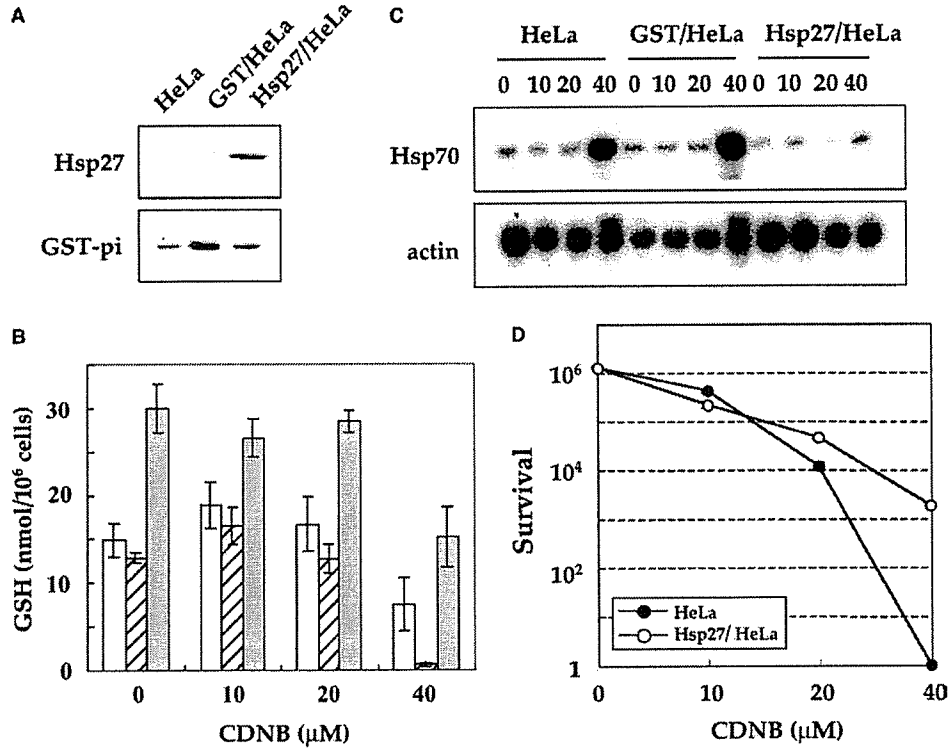


Fig. 4. Hsp27 reduces oxidative stress caused by CDNB. (A) HeLa cells were stably transfected with GST-pi expression vector or Hsp25 expression vector. Levels of Hsp25 and GST-pi were determined by Western blot analysis. (B) Cells were treated with 0, 10, 20 and 40 μM of CDNB for 8 h, and levels of GSH were measured. Means and S.D. of three independent experiments are shown. Open bar, HeLa; hatched bar, GST/HeLa; gray bar, Hsp27/HeLa. (C) Cells treated as described in B were harvested, and total RNAs were isolated from the cells and Northern blot analysis was performed. Representative data are shown from three experiments. (D) HeLa and Hsp27/HeLa cells were incubated in the presence of 0, 10, 20 or 40 μM CDNB for 24 h, and replated in dishes containing normal medium for 10 days. Means of three independent experiments of cell survivals are shown. S.D. are too small to be shown.

Electrophiles cause oxidative stress with rapid reduction of cellular glutathione level [21]. To cope with electrophiles and oxidants, cells induce phase 2 enzymes such as glutathione *S*-transferase and NAD(P)H:quinone oxidoreductase [22,23] by activating Nrf2 transcription factor [24,25]. Induction of these enzymes is accompanied by elevation of intracellular glutathione levels [26,27]. In addition to Nrf2 activation, we showed here that HSF1 is activated by electrophiles. This result might be expected because diamide and menadione, which induce oxidation of protein thiols by rapidly forming GSSG with subsequent GSH depletion, activate HSF1 [28,29]. The oxidation of protein thiols may cause denaturation of proteins, resulting in the formation of a state with similar properties to the thermally denatured state [30]. Here, we directly showed that overexpression of Hsp27 reduces toxic effects on cells, probably by increasing cellular GSH level. Because Hsp27 is a major inducible protein after feeding, it may play significant roles in suppressing toxic effects of xenobiotic chemicals in food.

*Acknowledgements:* We are grateful to Dr. M. Parmely for a protocol for DEM injection into mice. This work was supported in part by Grants-in-Aid for Scientific Research (B) (C), and on Priority Area-Cell Cycle, Life of proteins, and Cancer, from the Ministry of Education, Culture, Sports, Science and Technology, Japan, the Naitoh Foundation, and the Mochida Foundation.

## References

[1] Lindquist, S. and Craig, E.A. (1988) Annu. Rev. Genet. 22, 631–677.
[2] Morimoto, R.I. (1998) Genes Dev. 12, 3788–3796.
[3] Bukau, B. and Horwich, A.L. (1998) Cell 92, 351–366.
[4] Mehlen, P., Kretz-Remy, C., Preville, X. and Arrigo, A.P. (1996) EMBO J. 15, 2695–2706.
[5] Locke, M., Noble, E.G. and Atkinson, B.G. (1990) Am. J. Physiol. 258, C723–C729.
[6] Salo, D.C., Donovan, C.M. and Davies, K.J. (1991) Free Radic. Biol. Med. 11, 239–246.
[7] Blake, M.J., Udelsman, R., Feulner, G.J., Norton, D.D. and Holbrook, N.J. (1991) Proc. Natl. Acad. Sci. USA 88, 9873–9877.
[8] Udelsman, R., Blake, M.J., Stagg, C.A., Li, D.G., Putney, D.J. and Holbrook, N.J. (1993) J. Clin. Invest. 91, 465–473.
[9] Zucker, S.D. and Gollan, J.L. (1995) in: Physiology of the Liver (Haubrich, W.S., Schaffner, F. and Berk, J.E., Eds.) Gastroenterology, Vol. 3, pp. 1858–1905, W.B. Saunders Company, Pennsylvania.
[10] Jakoby, W.B. and Ziegler, D.M. (1990) J. Biol. Chem. 265, 20715–20718.
[11] Inouye, S., Katsuki, K., Izu, H., Fujimoto, M., Sugahara, K., Yamada, S., Shinkai, Y., Oka, Y., Katoh, Y. and Nakai, A. (2003) Mol. Cell. Biol. 23, 5882–5895.
[12] Nakai, A., Kawazoe, Y., Tanabe, M., Nagata, K. and Morimoto, R.I. (1995) Mol. Cell. Biol. 15, 5168–5178.
[13] Izu, H., Inouye, S., Fujimoto, M., Shiraishi, K., Naito, K. and Nakai, A. (2004) Biol. Reprod. 70, 18–24.

[14] Katoh, Y., Fujimoto, M., Nakamura, K., Inouye, S., Sugahara, K., Izu, H. and Nakai, A. (2004) FEBS Lett. 565, 28–32.
[15] Mannervik, B., Alin, P., Guthenberg, C., Jensson, H., Tahir, M.K., Warholm, M. and Jornvall, H. (1985) Proc. Natl. Acad. Sci. USA 82, 7202–7206.
[16] Wang, F., Wang, L.Y., Wright, D. and Parmely, M.J. (1999) Infect. Immun. 67, 5409–5416.
[17] Parmely, M.J., Wang, F. and Wright, D. (2001) Infect. Immun. 69, 2621–2629.
[18] Blake, M.J., Gershon, D., Fargnoli, J. and Holbrook, N.J. (1990) J. Biol. Chem. 265, 15275–15279.
[19] Dhahbi, J.M., Mote, P.L., Tillman, J.B., Walford, R.L. and Spindler, S.R. (1997) J. Nutr. 127, 1758–1764.
[20] Dhahbi, J.M., Cao, S.X., Tillman, J.B., Mote, P.L., Madore, M., Walford and R.L., Spindler (2001) Biochem. Biophys. Res. Commun. 284, 335–339.
[21] Deneke, S.M. and Fanburg, B.L. (1989) Am. J. Physiol. 257, L163–L173.
[22] Prochaska, H.J. and Talalay, P. (1988) Cancer Res. 48, 4776–4782.
[23] Prestera, T., Holtzclaw, W.D., Zhang, Y. and Talalay, P. (1993) Proc. Natl. Acad. Sci. USA 90, 2965–2969.
[24] Itoh, K., Chiba, T., Takahashi, S., Ishii, T., Igarashi, K., Katoh, Y., Oyake, T., Hayashi, N., Satoh, K., Hatayama, I., Yamamoto, M. and Nabeshima, Y. (1997) Biochem. Biophys. Res. Commun. 236, 313–322.
[25] Ishii, T., Itoh, K., Takahashi, S., Sato, H., Yanagawa, T., Katoh, Y., Bannai, S. and Yamamoto, M. (2000) J. Biol. Chem. 275, 16023–16029.
[26] Bannai, S. (1984) J. Biol. Chem. 259, 2435–2440.
[27] Deneke, S.M., Baxter, D.F., Phelps, D.T. and Fanburg, B.L. (1989) Am. J. Physiol. 257, L265–L271.
[28] Freeman, M.L., Borrelli, M.J., Syed, K., Senisterra, G., Stafford, D.M. and Lepock, J.R. (1995) J. Cell. Physiol. 164, 356–366.
[29] McDuffee, A.T., Senisterra, G., Huntley, S., Lepock, J.R., Sekhar, K.R., Meredith, M.J., Borrelli, M.J., Morrow, J.D. and Freeman, M.L. (1997) J. Cell. Physiol. 171, 143–151.
[30] Freeman, M.L., Huntley, S.A., Meredith, M.J., Senisterra, G.A. and Lepock, J. (1997) Cell Stress Chaperones 2, 191–198.

Available online at www.sciencedirect.com
SCIENCE DIRECT®
ELSEVIER
Cancer Letters 208 (2004) 115–122
CANCER Letters
www.elsevier.com/locate/canlet

# Integrin-linked kinase (ILK) regulation of the cell viability in PTEN mutant glioblastoma and in vitro inhibition by the specific COX-2 inhibitor NS-398

Soichi Obara[a,b,*], Masanori Nakata[c], Hideo Takeshima[a], Hideki Katagiri[d], Tomoichiro Asano[e], Yoshitomo Oka[d], Ikuro Maruyama[b], Jun-ichi Kuratsu[a]

[a]*Faculty of Medicine, Department of Neurosurgery, Kagoshima University, 8-35-1 Sakuragaoka, Kagoshima 890-8520, Japan*
[b]*Faculty of Medicine, Department of Laboratory and Molecular Medicine, Kagoshima University, 8-35-1 Sakuragaoka, Kagoshima 890-8520, Japan*
[c]*Department of Physiology, Jichi Medical School, Minamikawachi, Kawachi, Tochigi 329-0498, Japan*
[d]*Division of Molecular Metabolism and Diabetes, Department of Internal Medicine, Tohoku University Graduate School of Medicine Seiryo-machi, Sendai, 980-8574, Japan*
[e]*Faculty of Medicine, Department of Internal Medicine, University of Tokyo, 7-3-1, Hongo, Bunkyo-ku, Tokyo 113-8655, Japan*

Received 10 November 2003; received in revised form 12 November 2003; accepted 13 November 2003

**Abstract**

We report the increased activity and expression of the ILK protein in human glioblastomas and demonstrate that ILK activity is regulated by PTEN. The transfection of wild type-PTEN into the glioblastoma cell line U-251 MG altered the localization of ILK in the cell membrane; transfection with PTEN down-regulated PKB/Akt-Ser-473 phosphorylation via the inhibition of ILK-signaling. Our results suggest that ILK is critical for the PTEN-sensitive regulation of PKB/Akt-dependent cell survival. The selective COX-2 inhibitor NS-398 was found capable of down-regulating ILK and PKB/Akt phosphorylation. Our data indicate that inhibition of ILK signaling may be beneficial in the treatment of PTEN-deficient glioblastoma.


*Keywords:* Glioblastoma; ILK; PTEN; PKB/Akt-Serine 473; NS-398

## 1. Introduction

Glioblastoma is the most common and the most malignant tumor of the human central nervous system. Despite extensive clinical trials, a good clinical outcome has remained an elusive goal [1,2]. The success of treatment is hampered by factors such as the rapid growth, remarkable genetic and biological heterogeneity, and high degree of infiltration of these neoplasms [3,4]. The mechanisms by which tumor cells survive apoptosis induced by cytotoxic treatment modalities remain unclear. Growth or angiogenic factors, cytokines, and a diverse array of parallel and overlapping signaling pathways are involved in

* Corresponding author. Address: Faculty of Medicine, Department of Neurosurgery, Kagoshima University, 8-35-1 Sakuragaoka, Kagoshima 890-8520, Japan. Tel.: +81-99-275-5437; fax: +81-99-275-2629.
*E-mail address:* sochian@ta2.so-net.ne.jp (S. Obara).

0304-3835/$ - see front matter © 2003 Elsevier Ireland Ltd. All rights reserved.
doi:10.1016/j.canlet.2003.11.020

the regulation of DNA repair and apoptosis. Identifying and ultimately targeting the molecules by which gliomas resist cytotoxic agents will have a strong impact on future treatment strategies.

PTEN, the phosphatase and tensin homolog deleted from chromosome 10, (also known as the mutated gene in multiple advanced cancers, MMAC1, and as the TGF-regulated and epithelial cell-enriched phosphatase, TEP1) was identified as a tumor suppressor gene located on chromosome 10q23 [5,6,7]. Loss of heterozygosity (LOH) at this locus is observed at a high frequency in a wide variety of human cancers including glioblastomas, melanomas, and carcinomas of the prostate, breast, lung, and head and neck [8–13]. PTEN is a lipid phosphatase that dephosphorylates 3D of phosphatidyliositol 3.4.5 triphosphate (PI (3, 4, 5) P3), a product of PI3-kinase. The disruption of PTEN results in the serum- and anchorage-independent activation of PKB/Akt probably induced by increased levels of PI (3, 4, 5) P3 [14–16]. PKB/Akt suppresses apoptosis via several possible downstream effectors including phosphorylation and inactivation of BAD [17], or repression of the forkhead transcription factor [18]. The disruption of PTEN leads not only to the suppression of apoptosis, but also to cell-cycle acceleration via GSK-3 and CyclinD [15].

Integrin-linked kinase (ILK) was identified by the yeast two-hybrid system as a serine/threonine kinase that interacts with the β1 integrin subunit [19]. ILK possesses a number of oncogenic properties including the inhibition of apoptosis and the acceleration of tumor cell invasion [20,21]. It has also been shown to phosphorylate PKB/Akt on Ser-473 in vitro. Since this activity is sensitive to the level of PI (3, 4, 5) P3 [22], the disruption of PTEN would be expected to activate ILK, leading to PKB/Akt activation [23]. In fact, ILK and PKB/Akt are constitutively activated in PTEN-mutant prostate cancer cells. Furthermore, the expression of dominant-negative ILK dramatically inhibits serum- and anchorage-independent PKB/Akt phosphorylation as well as PKB/Akt kinase activity, and leads to G1 cell-cycle arrest and enhanced apoptosis [24].

In the present work, we demonstrate that ILK is activated in PTEN-deficient human glioblastoma cells. We also found that transfection of WT-PTEN into these cells inhibits ILK activity, changes the subcellular localization of ILK, and ultimately inhibits PKB/Akt kinase activity, enhanced cell-cycle arrest, and apoptosis. Our results demonstrate that ILK is critical for the PTEN-sensitive regulation of PKB/Akt-dependent cell-cycle progression and cell survival. ILK kinase activity is suppressed by non-steroidal anti-inflammatory drugs (NSAIDs) [25]. Therefore, we exposed U-251MG cells to the COX-2-specific inhibitor NS-398. Interestingly, PKB/Akt-Ser-473 phosphorylation and the ILK activity were significantly inhibited by the administration of NS-398. Our data suggest that the inhibition of ILK-signaling by NSAIDs may have therapeutic benefits in PTEN-deficient glioblastomas since the restoration of PTEN by a viral vector is clinically difficult. Targeting the downstream of signal transduction pathways involved in the biology of tumor cells may represent a novel therapeutic approach.

## 2. Materials and methods

*Brain tumor specimens and tumor cell lines.* Glioma tissue specimens, obtained from patients who underwent surgery at The Department of Neurosurgery, Kagoshima University, were immediately frozen in liquid nitrogen. Sections from all samples were histologically evaluated by board-certified neuropathologists and classified according to the WHO grading system.

The human glioblastoma cell line U-251 MG was obtained as previously described [26]. The cell was cultured in Dulbecco's modified Eagle's medium (DMEM)(Gibco BRL, Grand Island, NY) supplemented with 10% fetal bovine serum at 37 °C in the presence of 95% air and 5% $CO_2$.

*Gene expression.* Recombinant Ade-XCA-PTEN has been described [27]. After infecting the U251 cells with DMEM containing adenovirus (30 min, 37 °C), DMEM containing 10% FCS was added. The adenovirus was applied at a MOI of 5–20 pfu/cell, and incubated for 48 h. Ade-XCA-lacZ was used as a control since on the three post-infection days, >90% of U251 cells exposed to a MOI of 10–20 pfu/cells manifested Ade-XCA-lacZ gene expression.

*Immunohistochemistry.* Histological sections (5-μm in thickness) of formalin-fixed, paraffin-embedded surgical specimens were subjected to

immunohistochemical staining. After incubation with normal blocking serum, the sections were incubated overnight at 4 °C with primary anti-ILK polyclonal antibody (0.2 μg/ml; Upstate Biotechnology, Lake Placid, NY). For immunodetection we employed the Vectastatin ABC rabbit IgG kit (Vector Laboratories, Burlingame, CA) using diaminobenzidine as the chromogen. Negative control sections were stained first with nonspecific rabbit IgG at the same protein concentration as the primary anti-ILK antibody, followed by horseradish peroxidase-linked anti-rabbit secondary antibody. All sections were counterstained with hematoxylin.

*Immunoblot analysis.* The cultured cells were collected and briefly sonicated in a Modified Radioimmunoprecipitation (RIPA) buffer containing 50 mM Tris (pH 7.4), 1% NP-40, 1 mM EDTA, 0.25% Na-deoxycholate, 1 mM PMSF, 1 mM NaF, and 1 mM $Na_2VO_3$, and a protease inhibitor cocktail (BD Pharminogen, San Diego, CA). The cell membranes were collected by a Mem-PER Mammalian Membrane Protein Extraction Reagent Kit (PIERCE, Rockford, IL). Frozen tissue samples were homogenized in RIPA buffer.

Immunoblot analysis using the enhanced chemiluminescence (ECL) detection system (Amersham Pharmacia, Little Chalfont Buckinghamshire, England) were carried out as described [19,22]. The following antibodies were used: anti-PTEN (goat polyclonal; Santa Cruz Biotech, Santa Cruz, CA); anti-ILK (affinity-purified rabbit polyclonal and mouse monoclonal antibody; Upstate Biotechnology, Lake Placid, NY); anti-PKB/Akt-phospho-Ser-473 (rabbit polyclonal; Transduction Laboratories, Lexington, KY); anti-PKB/Akt (mouse monoclonal; Transduction Laboratories).

*ILK kinase assays.* The ILK kinase activity was determined in cell extracts by immunoprecipitation kinase assays [21,22]. Glutathione S-transferase (GST)-PKB/Akt-Ser-473 was used as a substrate for ILK in separate experiments, and the phosphorylated proteins were electrophoresed on 12% SDS/PAGE gels. GST-PKB/Akt was constructed with individual GST fusion proteins of the PKB/Akt c-terminal (aa 444–480) expressed in JM109, and purified on glutathione-sepharose beads. When GST-PKB/Akt-Ser-473 was the substrate, [$^{32}$P]ATP was used as the phosphate donor in the kinase assay; [$^{32}$P]PKB/Akt-Ser-473 was detected by autoradiography or phosphorimage analysis of the gels. Cold ATP was the phosphate donor in kinase assays; the proteins were electrotransferred from SDS/PAGE gels to immobilize poly-(vinylidene difluoride) membranes (Millipore, Bedford, MA). Phosphorylated GST-PKB/Akt-Ser-473 was then detected by Western blot using anti-PKB/Akt-phospho-Ser-473 antibody.

*Immunofluoresence microscopic analysis.* The cells were maintained for 24 h on fibronectin-coated four-well chamber slides (Asahi Techno Glass, Tokyo, Japan), transfected with the adenovirus vectors, and fixed with 4% paraformaldehyde (10 min) followed by 0.1% Triton × 100 in PBS (5 min). After washing with PBS, they were stained with anti-ILK rabbit polyclonal antibody (Upstate Biotechnology) and anti-paxillin mouse monoclonal antibody (Transduction Laboratories). After again washing with PBS, the cells were incubated with the second antibody (30 min) and examined using a confocal laser scanning microscope (Leica True Confocal Scanner 4D, Leica Lasertechnik GmbH, Heidelberg, Germany) as described previously [28].

*Cell viability.* To assay cell viability, a modified dimethyl-2-thiazolyl-2,5 -diphenyl-tetrazolium bromide (MTT) assay. Briefly, glioblastoma cells, seeded at a density of $1.0–2.0 \times 10^5$ cells per 60 mm-dish, were transfected with WT-PTEN or control vector, and treated for 48 h with or without NS-398 (CALBIOCEM, Darmstadt, Germany).

## 3. Results

Since the expression profile of ILK has not been documented in glioma cells to date, we first determined the constitutive expression of ILK in glioma tissues obtained at surgery. In human glioma tissues, the level of ILK protein was higher than in normal brain. Furthermore, ILK expression was correlated with the malignancy grade of the gliomas (Figs. 1 and 2A). The most malignant type, glioblastoma, manifested a higher level of ILK expression than did low-grade gliomas.

The up-regulation of ILK in glioma tissues was histologically verified by immunohistochemical analysis. Vascular endothelial cells, smooth muscle cells,

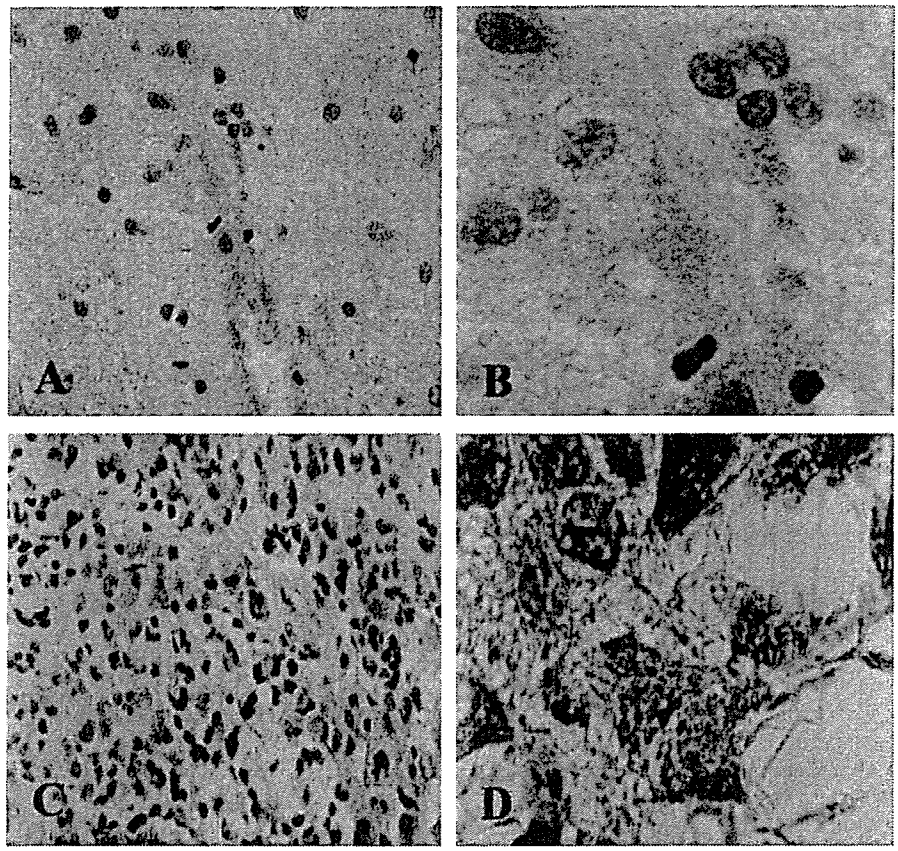


Fig. 1. Immunohistochemical detection of ILK in human glioma tissue. Low-grade astrocytoma and glioblastoma specimens were stained with primary anti-ILK polyclonal antibody followed by anti-rabbit secondary antibody. Vascular endothelial cells and pericytes were immunoreactive with anti-ILK antibody. Slight staining was detected in astrocytoma cells (A and B). Glioblastoma cells were stained strongly (C and D). Glioblastomas contained more ILK-positive cells than did low-grade astrocytomas. No staining was detected when control non-immune serum was used. Magnification: A and C × 200; B and D × 400.

and some tumor cells were immunoreactive with anti-ILK antibody in low-grade gliomas (Fig. 1A and B). On the other hand, the cytoplasm and cell surface were diffusely immunopositive for ILK in the majority of glioblastoma cells (Fig. 1C and D), suggesting that the increased level of ILK expression we observed was primarily attributable to the neoplastic glioma cells. In human glioma tissues, the level of ILK protein was higher than in normal brain. Furthermore, ILK expression was grossly correlated with the malignancy grade of the gliomas. The most malignant type, glioblastoma, manifested a higher level of ILK expression than low-grade gliomas by immunoblot analtysis (Fig. 2A).

To examine the biological relevance of ILK, PKB/AKT, and tumor suppressor PTEN in malignant glioma cells, we focused on how the PTEN status influenced the phosphorylation of PKB/AKT on Ser-473, and the expression level of ILK protein and it kinase activity. We experimented immunoprecipitated whole cell lysates with anti-ILK after transiently transfecting WT-PTEN into U-251 MG cells. Kinase assays using GST-PKB/AKT-C-terminal fusion protein as a substrate showed that restoration of PTEN leads not only to decreased PKB/AKT-Ser-473 phosphorylation but also to decreased ILK level and its activity (30% of mock stimulation; Fig. 2B and C).

As there is a direct association between ILK and paxillin with an LD1 motif, and co-localization in focal adhesions [29], we next examined whether decreased ILK activity affects the subcellular

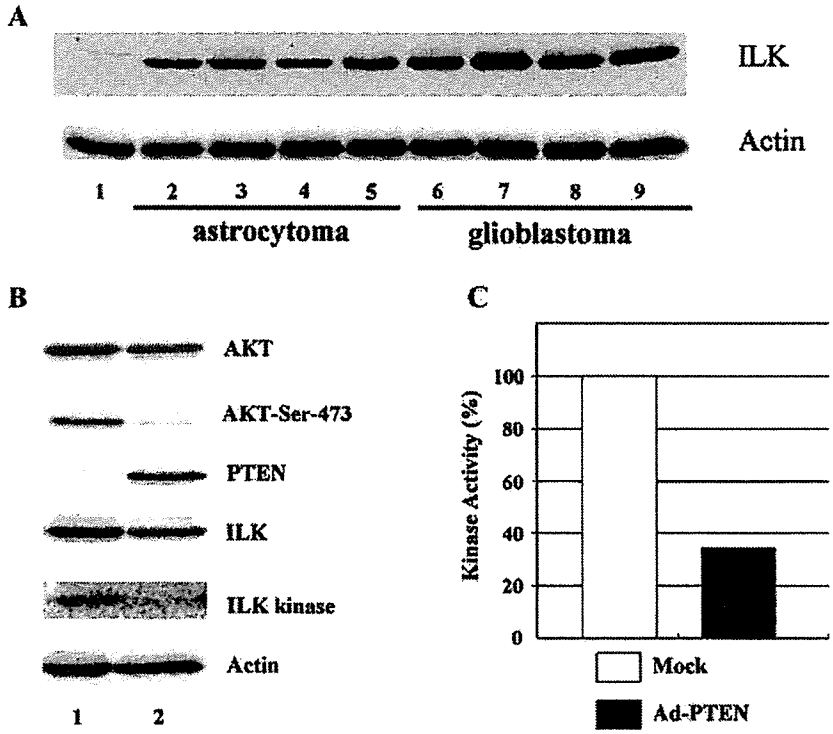


Fig. 2. Expression of ILK in glioma tissue specimens. Lane 1, normal human brain (CLONTECH). Lanes 2–5, human low-grade glioma tissues. Lanes 6–9, human glioblastoma tissues. The immunoblot with anti-actin (bottom) confirms equal loading of protein in each lane (A). Biological relevance of ILK, PKB/AKT, and tumor suppressor PTEN in malignant glioma cells. All cell lysates (500 mg protein) were immune-precipitated with anti-ILK antibody and kinase assays were performed using GST-PKB/AKT-C-terminal fusion protein as a substrate after transiently transfecting optimal MOI of PTEN adenovirus plasmid (20 MOI) into U-251 MG cells. Restoration of PTEN (lane 2) leads not only to decreased PKB/AKT-Ser-473 phosphorylation but also to decreased ILK level and its activity (30% of mock stimulation) (B). Densitometic analysis of ILK kinase. The intensity of immunoreactivity was measured by densitometry using the NIH-IMAGE image analysis software package (open bar, control adenovirus plasmid; solid bar, PTEN adenovirus plasmid) (C).

localization of ILK in glioblastoma cells. As expected, transfection with WT-PTEN not only inhibited ILK activity but also disrupted ILK localization on the cell membrane (Fig. 3A). To semi-quantitatively evaluate the shift of ILK from the cell membrane to the cytoplasm under different experimental conditions, we subjected equal amounts of membrane-bound and cytosolic proteins to immunoblot for ILK. As shown in Fig. 3B, a significant ILK shift from the membranous fraction to the cytoplasmic fraction was detected in PTEN-transfected U-251MG cells.

Restoration of PTEN produced cell-cycle arrest by inhibiting ILK activity in a variety of PTEN-deficient cell-lines such as prostate cancer lines [24]. Interestingly ILK activity has been shown to be inhibited by the administration of nonsteroidal anti-inflammatory drugs (NSAIDs) that can block both COX-1 and COX-2 [25]. Therefore, it is possible that the COX inhibitor suppresses the proliferation of glioma cells by inhibiting ILK activity regardless of the presence of wild-type PTEN.

We next compared the biological effect on cell proliferation of the specific COX-2 inhibitor NS-398 and of PTEN transfection. Interestingly, exposure to NS-398 (10 μM) resulted in a decrease in cell proliferation (Fig. 4A) that was comparable to that induced by PTEN-transfection. Immunoblot analysis demonstrated that phosphorylation of PKB/AKT-Ser-473 and ILK activities were significantly inhibited by cell exposure to NS-398 (Fig. 4B).

Our data demonstrate that in glioblastoma cells, like restoration of PTEN or exposure to NS-398, ILK induces decrease in cell proliferation. Therefore,

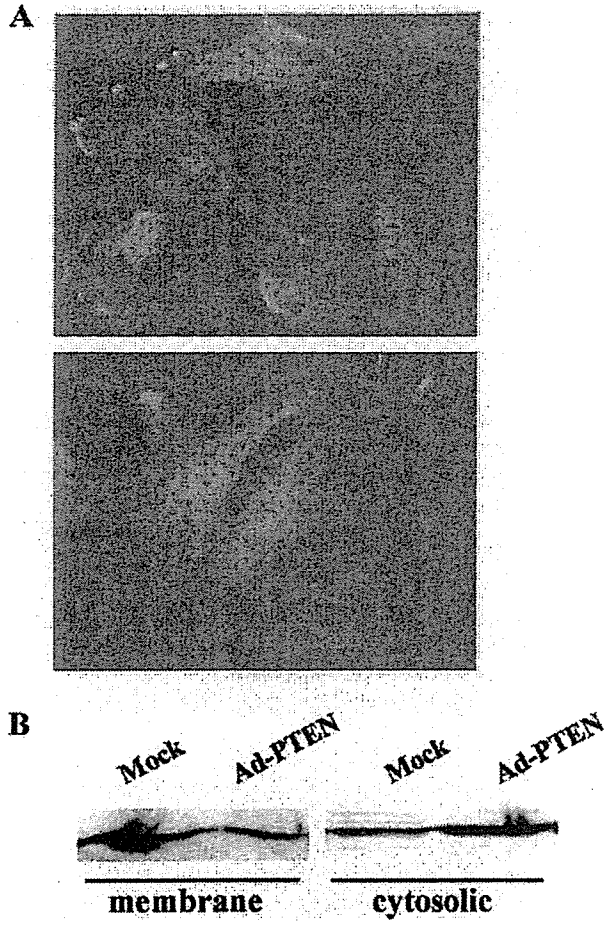


Fig. 3. Subcellular distribution of ILK. Immunofluorescence staining with ILK antibody of U-251 MG glioblastoma cells. After transfection with Mock Ad-LacZ, fluorescence-labeled ILK were identified in the cell membrane (upper panel). Transfection with Ad-PTEN resulted in disorganized ILK-staining in the cell membrane (lower panel) (A). Distribution of ILK in subcellular fractions of plasma membrane of U251 MG cells. Under different experimental conditions, equal amounts of membrane-bound and cytosolic proteins were Immunoblotted for ILK. Transfection with Ad-PTEN was associated with an attenuation of the presence of ILK in the membrane and its appearance in the cytoplasmic fraction (B).

the inhibition of ILK may represent a novel means of inhibiting the growth and progression of PTEN-mutant tumors.

## 4. Discussion

Increased ILK activity is correlated with the malignancy grade of several types of human tumors including breast, prostate, and colon carcinomas [30]. In the present work, we demonstrated the expression of ILK protein in human glioma cells. As shown by immunohistochemical and Immunoblot analysis, compared to low-grade gliomas, those of high grade expressed elevated levels of ILK protein. This is the first demonstration that in human glioblastoma cell line, ILK activity is constitutively activated. Furthermore, we found that the down-regulation of ILK activity by PTEN was related to changes in the localization of ILK from the cell membrane to the cytoplasm and ILK detached from focal adhesion plaques. ILK interacts with the cytoplasmic domains of β1 and β3 integrins via its C-terminal domain [31]. It was recruited to focal adhesions on extracellular matrix proteins and the kinase activity of ILK

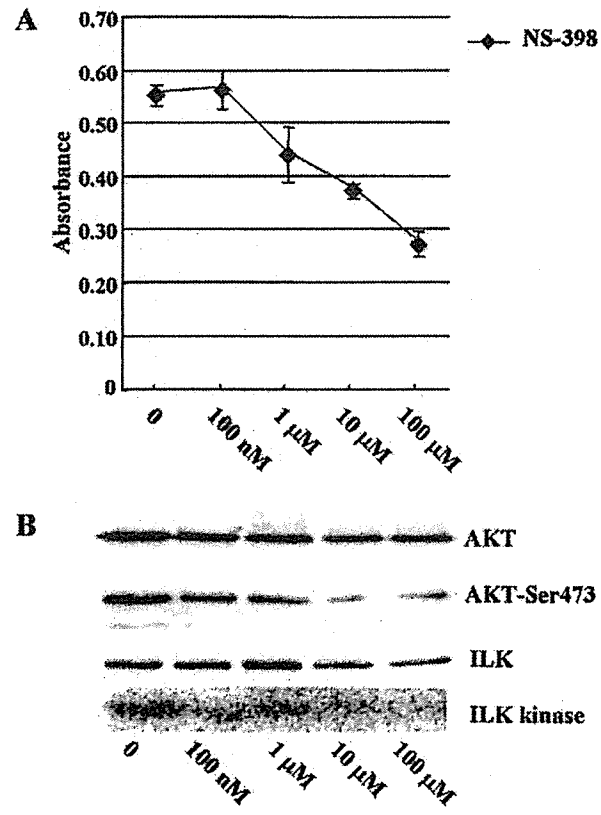


Fig. 4. Biological effect of the Cox2 inhibitor NS-398 in U-251 MG cells. To determine the MTT-induced reduction of cell viability, U-251 MG cells were incubated in 96-well microplates and exposed for 2 days to different concentrations of NS-398 (A). The results are given as the mean ± SD ($n = 3$). Immunoblot analysis of PKB/Akt-Ser-473 phosphorylation and in vitro kinase assay of ILK in NS-398-treated U-251 MG cells (B).

correlated with its anchoring on the cell membrane [29]. The activation of ILK in PTEN-null glioblastoma cells is presumably due to increased PI (3, 4, 5) P3 levels in these cells, although it is possible that ILK activation is due to dysregulation of other PTEN targets such as FAK [32]. Results from in vivo experiments suggested a role for PTEN in cell–cell and cell–matrix interactions and motility. Mouse embryos lacking PTEN exhibit severely disorganized blastocysts, suggesting that the expression of PTEN is required for proper cell–cell signaling. Furthermore, mutations in PTEN predominate in advanced invasive tumors and are present in about 72% of glioblastomas [33]. These findings suggest a role for PTEN in metastatic progression and are consistent with its putative role in adhesion and motility. As ILK overexpression resulted not only in cell transformation but also in increased metastasis in in vitro models [19,31,34,35], it is possible that ILK mediates many of the tumor suppressor functions of PTEN.

COX-2 is overexpressed in several tumor cells including glioma cells, and the COX-2 inhibitor suppressed the growth of these tumors [36,37]. Furthermore, ILK kinase activity was suppressed by NSAIDs such as ASA and Sulindac [25]. These lines of evidence suggest that the activation of ILK activity in cells containing COX-2 plays an important role in cell-cycle progression in these cells. Here we demonstrated that exposure of U-251MG cells to 20 μM NS-398 significantly inhibited ILK activity and PKB/AKT-Ser473 phosphorylation. Using the MTT cell proliferation assay, we also showed that tumor cell proliferation was inhibited.

Our findings indicate that the inactivation of a tumor suppressor results in the dysregulated activation of immediate downstream effectors. Their inhibition may represent selective and alternative means of treating tumors harboring mutations in the tumor suppressor genes. We demonstrated that the inhibition of ILK in glioblastoma cells induces decrease in cell proliferation. Our results suggest that the effects of ILK inhibition are specific for properties underlying malignant transformation. Therefore, targeting the ILK signal transduction pathways involved in the biology of glioblastoma cells may represent a therapeutic approach in the treatment of PTEN-deficient glioblastomas.

## Acknowledgements

This research was supported in part by grants from the Ministry of Education, Science and Culture of Japan (to Masanori Nakata, Ikuro Maruyama, Jun-ichi Kuratsu, Yoshitomo Oka,) and a Jichi Medical School Young Investigator Award (to Masanori Nakata).

## References

[1] F.W. Kreth, P.C. Warnke, R. Scheremet, C.B. Ostertag, Surgical resection and radiation therapy versus biopsy and radiation therapy in the treatment of glioblastoma multiforme, J. Neurosurg. 78 (1993) 762–766.
[2] F.W. Kreth, A. Berlis, V. Spiropoulou, M. Faist, R. Scheremet, R. Rossner, et al., The role of tumor resection in the treatment of glioblastoma multiforme in adults, Cancer 86 (1999) 2117–2123.
[3] D.C. Lyden, W.P. Mason, J.L. Finlay, The expanding role of chemotherapy for pediatric supratentorial malignant gliomas, J. Neurooncol. 28 (1996) 185–191.
[4] T.W. Trask, R.P. Trask, E. Aguilar-Cordova, H.D. Shine, P.R. Wyde, J.C. Goodman, et al., Phase I study of adenoviral delivery of the HSV-tk gene and ganciclovir administration in patients with current malignant brain tumors, Mol. Ther. 1 (2000) 195–203.
[5] D.M. Li, H. Sun, TEP1, encoded by a candidate tumor suppressor locus, is a novel protein tyrosine phosphatase regulated by transforming growth factor beta, Cancer Res. 57 (1997) 2124–2129.
[6] J. Li, C. Yen, D. Liaw, K. Podsypanina, S. Bose, S.I. Wang, et al., PTEN, a putative protein tyrosine phosphatase gene mutated in human brain, breast, and prostate cancer, Science 275 (1997) 1943–1947.
[7] P.A. Steck, M.A. Pershouse, S.A. Jasser, W.K. Yung, H. Lin, A.H. Ligon, et al., Identification of a candidate tumour suppressor gene, MMAC1, at chromosome 10q23.3 that is mutated in multiple advanced cancers, Nat. Genet. 15 (1997) 356–362.
[8] B.K. Rasheed, T.T. Stenzel, R.E. McLendon, R. Parsons, A.H. Friedman, H.S. Friedman, et al., PTEN gene mutations are seen in high-grade but not in low-grade gliomas, Cancer Res. 57 (1997) 4187–4190.
[9] W. Liu, C.D. James, L. Frederick, B.E. Alderete, R.B. Jenkins, PTEN/MMAC1 mutations and EGFR amplification in glioblastomas, Cancer Res. 57 (1997) 5254–5257.
[10] P. Guldberg, P. thor Straten, A. Birck, V. Ahrenkiel, A.F. Kirkin, J. Zeuthen, Disruption of the MMAC1/PTEN gene by deletion or mutation is a frequent event in malignant melanoma, Cancer Res. 57 (1997) 3660–3663.
[11] P. Cairns, K. Okami, S. Halachmi, N. Halachmi, M. Esteller, J.G. Herman, et al., Frequent inactivation of PTEN/MMAC1 in primary prostate cancer, Cancer Res. 57 (1997) 4997–5000.

[12] D.H. Teng, R. Hu, H. Lin, T. Davis, D. Iliev, C. Frye, et al., MMAC1/PTEN mutations in primary tumor specimens and tumor cell lines, Cancer Res. 57 (1997) 5221–5225.
[13] T. Kohno, M. Takahashi, R. Manda, J. Yokota, Inactivation of the PTEN/MMAC1/TEP1 gene in human lung cancers, Genes Chromosomes Cancer 22 (1998) 152–156.
[14] V. Stambolic, A. Suzuki, J.L. de la Pompa, G.M. Brothers, C. Mirtsos, T. Sasaki, et al., Negative regulation of PKB/Akt-dependent cell survival by the tumor suppressor PTEN, Cell 95 (1998) 29–39.
[15] H. Sun, R. Lesche, D.M. Li, J. Liliental, H. Zhang, J. Gao, et al., PTEN modulates cell cycle progression and cell survival by regulating phosphatidylinositol 3,4,5,-trisphosphate and Akt/protein kinase B signaling pathway, Proc. Natl Acad. Sci. USA 96 (1999) 6199–6204.
[16] S. Ramaswamy, N. Nakamura, F. Vazquez, D.B. Batt, S. Perera, T.M. Roberts, W.R. Sellers, Regulation of G1 progression by the PTEN tumor suppressor protein is linked to inhibition of the phosphatidylinositol 3-kinase/Akt pathway, Proc. Natl Acad. Sci. USA 96 (1999) 2110–2115.
[17] S.R. Datta, H. Dudek, X. Tao, S. Masters, H. Fu, Y. Gotoh, M.E. Greenberg, Akt phosphorylation of BAD couples survival signals to the cell-intrinsic death machinery, Cell 91 (1997) 231–241.
[18] A. Brunet, A. Bonni, M.J. Zigmond, M.Z. Lin, P. Juo, L.S. Hu, et al., Akt promotes cell survival by phosphorylating and inhibiting a Forkhead transcription factor, Cell 96 (1999) 857–868.
[19] G.E. Hannigan, C. Leung-Hagesteijn, L. Fitz-Gibbon, M.G. Coppolino, G. Radeva, J. Filmus, et al., Regulation of cell adhesion and anchorage-dependent growth by a new beta 1-integrin-linked protein kinase, Nature 379 (1996) 91–96.
[20] S. Attwell, C. Roskelley, S. Dedhar, The integrin-linked kinase (ILK) suppresses anoikis, Oncogene 19 (2000) 3811–3815.
[21] A.A. Troussard, P. Costello, T.N. Yoganathan, S. Kumagai, C.D. Roskelley, S. Dedhar, The integrin linked kinase (ILK) induces an invasive phenotype via AP-1 transcription factor-dependent upregulation of matrix metalloproteinase 9 (MMP-9), Oncogene 19 (2000) 5444–5452.
[22] M. Delcommenne, C. Tan, V. Gray, L. Rue, J. Woodgett, S. Dedhar, Phosphoinositide-3-OH kinase-dependent regulation of glycogen synthase kinase 3 and protein kinase B/AKT by the integrin-linked kinase, Proc. Natl Acad. Sci. USA 95 (1998) 11211–11216.
[23] S. Persad, S. Attwell, V. Gray, N. Mawji, J.T. Deng, D. Leung, et al., Regulation of protein kinase B/Akt-serine 473 phosphorylation by integrin-linked kinase: critical roles for kinase activity and amino acids arginine 211 and serine 343, J. Biol. Chem. 276 (2001) 27462–27469.
[24] S. Persad, S. Attwell, V. Gray, M. Delcommenne, A. Troussard, J. Sanghera, S. Dedhar, Inhibition of integrin-linked kinase (ILK) suppresses activation of protein kinase B/Akt and induces cell cycle arrest and apoptosis of PTEN-mutant prostate cancer cells, Proc. Natl. Acad. Sci. USA 97 (2000) 3207–3212.
[25] A. Marotta, C. Tan, V. Gray, S. Malik, S. Gallinger, J. Sanghera, et al., Dysregulation of integrin-linked kinase (ILK) signaling in colonic polyposis, Oncogene 20 (2001) 6250–6257.
[26] J. Kuratsu, K. Sato, Y. Saitoh, H. Takeshima, M. Morioka, Y. Ushio, The mechanism of growth-regulation of glioma cells by trapidil, J. Neurooncol. 23 (1995) 201–206.
[27] H. Ono, H. Katagiri, M. Funaki, M. Anai, K. Inukai, Y. Fukushima, et al., Regulation of phosphoinositide metabolism, Akt phosphorylation, and glucose transport by PTEN (phosphatase and tensin homolog deleted on chromosome 10) in 3T3-L1 adipocytes, Mol. Endocrinol. 15 (2001) 1411–1422.
[28] I. Kitajima, K. Kawahara, N. Hanyu, H. Shin, T. Tokioka, Y. Soejima, et al., Enhanced E-cadherin expression and increased calcium-dependent cell–cell adhesion in human T-cell leukemia virus type I Tax-expressing PC12 cells, J. Cell Sci. 109 (Pt3) (1996) 609–617.
[29] F. Li, Y. Zhang, C. Wu, Integrin-linked kinase is localized to cell-matrix focal adhesions but not cell-cell adhesion sites and the focal adhesion localization of integrin-linked kinase is regulated by the PINCH-binding ANK repeats, J. Cell Sci. 112 (Pt 24) (1999) 4589–4599.
[30] S.C. Wang, K. Makino, W. Xia, J.S. Kim, S.A. Im, H. Peng, et al., DOC-2/hDab-2 inhibits ILK activity and induces anoikis in breast cancer cells through an Akt-independent pathway, Oncogene 20 (2001) 6960–6964.
[31] G.E. Hannigan, J. Bayani, R. Weksberg, B. Beatty, A. Pandita, S. Dedhar, J. Squire, Mapping of the gene encoding the integrin-linked kinase, ILK, to human chromosome 11 p15.5–p15.4, Genomics 42 (1997) 177–179.
[32] M. Tamura, J. Gu, K. Matsumoto, S. Aota, R. Parsons, K.M. Yamada, Inhibition of cell migration, spreading, and focal adhesions by tumor suppressor PTEN, Science 280 (1998) 1614–1617.
[33] H. Lin, M.L. Bondy, L.A. Langford, K.R. Hess, G.L. Delclos, X. Wu, et al., Allelic deletion analyses of MMAC/PTEN and DMBT1 loci in gliomas: relationship to prognostic significance, Clin. Cancer Res. 4 (1998) 2447–2454.
[34] G. Radeva, T. Petrocelli, E. Behrend, C. Leung-Hagesteijn, J. Filmus, J. Slingerland, S. Dedhar, Overexpression of the integrin-linked kinase promotes anchorage-independent cell cycle progression, J. Biol. Chem. 272 (1997) 13937–13944.
[35] D.E. White, R.D. Cardiff, S. Dedhar, W.J. Muller, Mammary epithelial-specific expression of the integrin-linked kinase (ILK) results in the induction of mammary gland hyperplasias and tumors in transgenic mice, Oncogene 20 (2001) 7064–7072.
[36] T. Shono, P.J. Tofilon, J.M. Bruner, O. Owolabi, F.F. Lang, Cyclooxygenase-2 expression in human gliomas: prognostic significance and molecular correlations, Cancer Res. 61 (2001) 4375–4381.
[37] T. Joki, O. Heese, D.C. Nikas, L. Bello, J. Zhang, S.K. Kraeft, et al., Expression of cyclooxygenase 2 (COX-2) in human glioma and in vitro inhibition by a specific COX-2 inhibitor, NS-398, Cancer Res. 60 (2000) 4926–4931.

Available online at www.sciencedirect.com

SCIENCE DIRECT

European Journal of Pharmacology 502 (2004) 243–252

www.elsevier.com/locate/ejphar

# Unique roles of G protein-coupled histamine $H_2$ and gastrin receptors in growth and differentiation of gastric mucosa

Yasushi Fukushima[a,*], Toshimitsu Matsui[b], Toshihito Saitoh[c], Masao Ichinose[d], Keisuke Tateishi[a], Takayuki Shindo[a], Midori Fujishiro[a], Hideyuki Sakoda[a], Nobuhiro Shojima[a], Akifumi Kushiyama[a], Satoru Fukuda[a], Motonobu Anai[a], Hiraku Ono[a], Masashi Oka[d], Yasuhito Shimizu[d], Hiroki Kurihara[a], Ryozo Nagai[a], Takashi Ishikawa[a], Tomoichiro Asano[a], Masao Omata[a]

[a]*Department of Internal Medicine, Graduate School of Medicine, University of Tokyo, 7-3-1 Hongo, Bunkyo-ku, Tokyo 113-8655, Japan*
[b]*Division of Hematology/Oncology, Department of Medicine, Kobe University School of Medicine, Kobe, Hyogo 650-0017, Japan*
[c]*Department of Internal Medicine, Tokyo Women's Medical University Daini Hospital, Arakawa-ku, Tokyo 116-8567, Japan*
[d]*Second Department of Internal Medicine, Wakayama Medical College, Kimiidera, Wakayama 640-0012, Japan*

Received 10 June 2004; received in revised form 20 August 2004; accepted 1 September 2004
Available online 1 October 2004

**Abstract**

Disruption of histamine $H_2$ receptor and gastrin receptor had different effects growth of gastric mucosa: hypertrophy and atrophy, respectively. To clarify the roles of gastrin and histamine $H_2$ receptors in gastric mucosa, mice deficient in both (double-null mice) were generated and analyzed. Double-null mice exhibited atrophy of gastric mucosae, marked hypergastrinemia and higher gastric pH than gastrin receptor-null mice, which were unresponsive even to carbachol. Comparison of gastric mucosae from 10-week-old wild-type, histamine $H_2$ receptor-null, gastrin receptor-null and double-null mice revealed unique roles of these receptors in gastric mucosal homeostasis. While small parietal cells and increases in the number and mucin contents of mucous neck cells were secondary to impaired acid production, the histamine $H_2$ receptor was responsible for chief cell maturation in terms of pepsinogen expression and type III mucin. In double-null and gastrin receptor-null mice, despite gastric mucosal atrophy, surface mucous cells were significantly increased, in contrast to gastrin-null mice. Thus, it is conceivable that gastrin-gene product(s) other than gastrin-17, in the stimulated state, may exert proliferative actions on surface mucous cells independently of the histamine $H_2$ receptor. These findings provide evidence that different G-protein coupled-receptors affect differentiation into different cell lineages derived from common stem cells in gastric mucosa.


*Keywords:* G protein; Histamine $H_2$; Double-null, mouse

## 1. Introduction

Recently, gene-targeting techniques have made it possible to generate mice deficient in a number of genes involved in gastric acid secretion (Friis-Hansen et al., 1998; Fukushima et al., 2003; Kobayashi et al., 2000; Koh et al., 1997; Langhans et al., 1997; Lloyd et al., 1997; Matsui et al., 2000; Nagata et al., 1996; Tanaka et al., 2002). Of these gene products, histamine $H_2$, gastrin, and muscarine $M_3$ receptors are direct targets of secretagogues and are involved in acid production in parietal cells. Targeted disruption of the histamine $H_2$ receptor caused hypertrophy of gastric mucosa due to marked hyperplasia of parietal, mucous neck and enterochromaffin-like (ECL) cells (Fukushima et al., 2003). Despite prominent hypergastrinemia, surface mucous cells were not as increased in number as downward migrating cells in histamine $H_2$ receptor-null mice (Fukushima et al., 2003). In contrast, gastrin receptor-null mice exhibited remarkable

* Corresponding author. Tel.: +81 3 3815 5411x33133; fax: +81 3 5803 1874.
*E-mail address:* fksm@mth.biglobe.ne.jp (Y. Fukushima).

0014-2999/$ - see front matter © 2004 Elsevier B.V. All rights reserved.
doi:10.1016/j.ejphar.2004.09.013

gastric mucosae atrophy accompanied by decreases in parietal and ECL cell numbers (Nagata et al., 1996). Although differences in pH values between wild-type mice and histamine $H_2$ receptor-null mice were minimal (Fukushima et al., 2003; Kobayashi et al., 2000), gastrin-dependent acid production was impaired in histamine $H_2$ receptor-null mice. In gastrin receptor-null mice, basal acid productions were lower than those in wild-type mice (Langhans et al., 1997; Nagata et al., 1996). In this study, to further clarify the distinct roles of histamine $H_2$ receptor and gastrin receptor in gastric mucosa, mice deficient in both the histamine $H_2$ and the gastrin receptors (double-null mice) were generated. We also analyzed gastric mucosa from aged histamine $H_2$ receptor-null mice and aged double-null mice. Herein, we present evidence that these different G-protein coupled-receptors mediate differentiation into different cell lineages derived from common stem cells in gastric mucosa.

## 2. Materials and methods

### 2.1. Mice

All animal experimental procedures were reviewed and approved by the Institutional Animal Care and Research Advisory Committee of the University of Tokyo. Mice deficient in histamine $H_2$ receptors were generated as described previously (Fukushima et al., 2003; Shindo et al., 2002).

### 2.2. Generation of mice deficient in both the histamine $H_2$ receptor and the gastrin receptor (double-null mice)

Histamine $H_2$ receptor-null mice and gastrin receptor-null mice with the genetic background of the 129/Sv×C57BL/6 hybrid were used (Fukushima et al., 2003; Nagata et al., 1996). Offspring obtained by crossing histamine $H_2$ receptor-null and gastrin receptor-null mice were confirmed to be heterozygous for both the histamine $H_2$ receptor and the gastrin receptor. These mice were then crossed and the offspring thus obtained were genotyped with PCR and/or Southern blot analysis using genomic DNA prepared from tail biopsies. Of these offspring, wild-type, histamine $H_2$ receptor-null, gastrin receptor-null and double-null mice were used for the following studies. Double-null mice appeared normal, were healthy into adulthood and both sexes were fertile.

### 2.3. Generation of polyclonal antibody against murine pepsinogen C

Polyclonal antibody against murine pepsinogen C was generated by a previously described method (Fukushima et al., 1993). The 100 carboxyl-terminal amino acids of murine pepsinogen C were fused to Glutathione *S*-transferase, which was used to immunize female New Zealand white rabbits. Serum collected from the immunized rabbits was passed through Affigel-10 beads, which had been cross-linked to Glutathione *S*-transferase. The flow-through was collected and passed through Afvfigel-10 beads, which had been cross-linked to the fusion protein. Antibody adsorbed to the beads was collected. This polyclonal antibody specifically recognizes chief cells in mouse oxyntic mucosa.

### 2.4. Histological analysis

Gastric specimens were fixed in 3% phosphate-buffered paraformaldehyde (pH 7.4), embedded in paraffin, and cut into 3 μm sections. The sections were stained with periodic acid-Schiff (PAS), hematoxylin and eosin, and examined under a light microscope. Paraffin-embedded gastric tissue sections were dewaxed and rehydrated with graded concentrations of ethanol. After treatment with 2% $H_2O_2$/phosphate buffered saline for 10 min, tissue sections were incubated with anti-pepsinogen C antibody, anti-histidine decarboxylase (HDC) polyclonal antibody, anti-$H^{(+)}/K^{(+)}$-ATPase monoclonal antibody (Fukushima et al., 1999), anti-type III mucin monoclonal antibody HIK1087 (Kanto-Kagaku, Japan) or normal rabbit or mouse immunoglobulin G (IgG) overnight at 4 °C. The sections were rinsed and then incubated for 30 min with biotinylated anti-rabbit or mouse IgG (1:400 dilution). The tissue sections were then rinsed and incubated for 30 min with peroxidase-labeled streptavidin (1:70 dilution). The slides were rinsed again in phosphate buffered saline and reacted with diaminobenzidine for 5 min at room temperature. Finally, the sections were rinsed and counterstained with hematoxylin.

### 2.5. Incorporation of the thymidine analog bromodeoxyuridine (BrdU)

BrdU (80 mg/kg BW(body weight)) was injected intraperitoneally into mice 2 h before sacrifice. Gastric tissues were removed and fixed in 3% phosphate-buffered paraformaldehyde. Immunohistochemistry with anti-BrdU monoclonal antibody was performed using paraffin-embedded sections from these samples.

### 2.6. Measurement of gastric pH

Wild-type and histamine $H_2$ receptor-null mice were fasted overnight with free access to water. At 1.5 h after subcutaneous injection of vehicle (0.5% methylcellulose), 10 mg/kg BW of famotidine, 10 mg/kg BW of pirenzepine dihydrochloride (a muscarine $M_1$ receptor antagonist) or 10 mg/kg BW of (*R*)-1-[2,3-dihydro-1-(2′ -methylphenacyl)-2-oxo-5-phenyl-1H-1,4-benzodiazepin-3-yl]-3-(3-methylphenyl)urea (YM022), a gastrin receptor antagonist, the mice were sacrificed and their stomachs were immediately excised. Gastric pH was measured using an ultra-thin pH monitor (Horiba, Japan).

### 2.7. Measurement of secretagogue induced acid secretion

Mice were maintained on anesthesia in chambers infused with oxygen gas saturated with diethylether. The stomach and duodenum were exposed via an epigastric midline incision. A tube inserted from the duodenum was placed in the gastric lumen. Stomachs were washed with 1 ml of prewarmed physiologic saline three times. After extraction of the tube and ligation of the pylorus, physiologic saline or secretagogue solution was administered peritoneally. A total of 10 mg/kg BW of histamine dihydrochloride, 0.05 mg/kg BW of carbachol or 0.1 mg/kg BW of gastrin-17 were administered, i.e. 2.5 ml/kg BW of physiologic saline as a control, histamine dihydrochloride solution (4 mg/ml), carbachol solution (0.02 mg/ml) or gastrin-17 solution (0.04 mg/ml). Thirty minutes after administration, the mice were sacrificed and their stomachs were excised. Gastric juice was collected with 1.5 ml of physiologic saline. Secreted gastric acid was measured by titrating the collected gastric juice to pH 7.0.

### 2.8. Statistical analysis

Quantitative values were expressed as means±S.E. Statistical significance was tested using the unpaired *t*-test (two tailed). A value of $P<0.05$ was considered significant.

## 3. Results

### 3.1. Comparison of gastric mucosae and serum gastrin levels of 10-week-old histamine $H_2$ receptor-null, gastrin receptor-null, double-null and wild-type mice

Stomachs from 10-week-old double-null mice weighed significantly less than those of 10-week-old wild-type mice

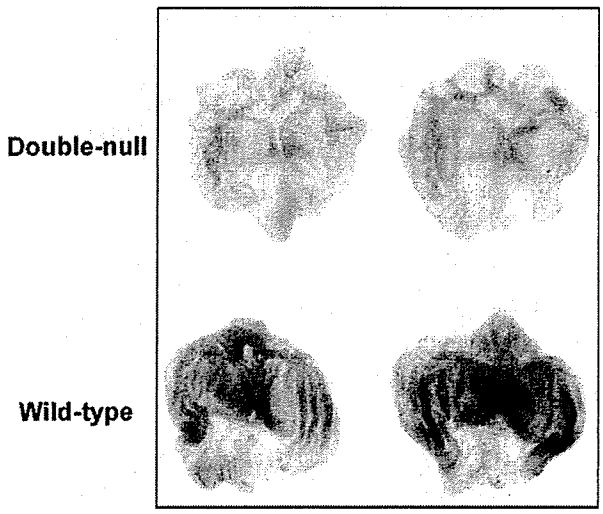


Fig. 1. Macroscopic views of stomachs from 10-week-old wild-type and double-null mice. The excised stomachs were opened along the greater curvature.

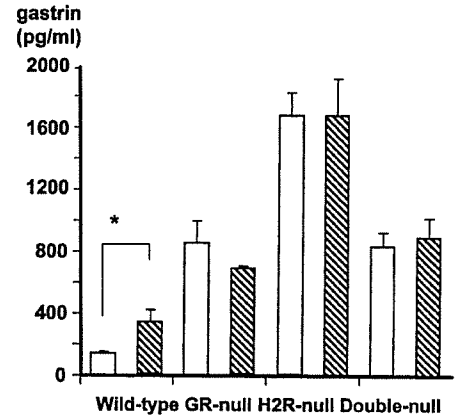


Fig. 2. Serum gastrin levels in wild-type, histamine $H_2$ receptor-null, gastrin receptor-null and double-null mice. Serum gastrin levels were measured in fasting (open bars) and fed states (hatched bars) in 10- to 12-week-old wild-type, histamine $H_2$ receptor-null (H2R-null), gastrin receptor-null (GR-null) and double-null mice. Data are presented as means±S.E. ($n$=15). *$P<0.0001$ between fasting and fed states.

(double-null 60.0±0.6 g/kg BW, wild-type 79.0±1.0 g/kg BW, $P<0.0001$). Macroscopically, oxyntic mucosae from double-null mice were more atrophic than those from wild-type mice (Fig. 1). Serum gastrin levels in double-null mice were significantly higher than those in wild-type mice, while being comparable to and lower than those in gastrin receptor-null mice and histamine $H_2$ receptor-null mice, respectively (Fig. 2). In addition, except in wild-type mice serum gastrin levels were not elevated by feeding (Fig. 2).

To explore the effects of disrupting gastrin receptor and histamine $H_2$ receptor genes, we examined oxyntic mucosae from the four types of mice at 10 weeks of age, PAS staining of gastric mucosa from 10-week-old double-null mice showed no hypertrophy of oxyntic mucosae in double-null mice (Fig. 3D).

In histamine $H_2$ receptor-null mice, oxyntic mucosal hypertrophy was attributable to hyperplasia of ECL, parietal and mucous neck cells, and parietal cells were small (Table 1). In some portions of oxyntic mucosae from histamine $H_2$ receptor-null mice, peculiar mucous neck cells full of mucin protruded into the gastric gland lumen. Despite marked hypergastrinemia surface mucous cells were not as increased in number as the downward migrating cells, resulting in a decreased percentage of surface mucous cells per gland in histamine $H_2$ receptor-null mice. These findings confirm our previous report on histamine $H_2$ receptor-null mice (Table 1, Fig. 3B) (Fukushima et al., 2003). However, on closer examination, we found the number of surface mucous cells to be significantly increased as compared to wild-type mice (Table 1).

In gastrin receptor-null mice, numbers of downward migrating cells were decreased as previously reported ($P<0.001$, vs. wild-type mice) (Table 1) (Nagata et al., 1996). Interestingly, surface mucous cell cells were increased in number as compared with wild-type mice (26.7±1.6

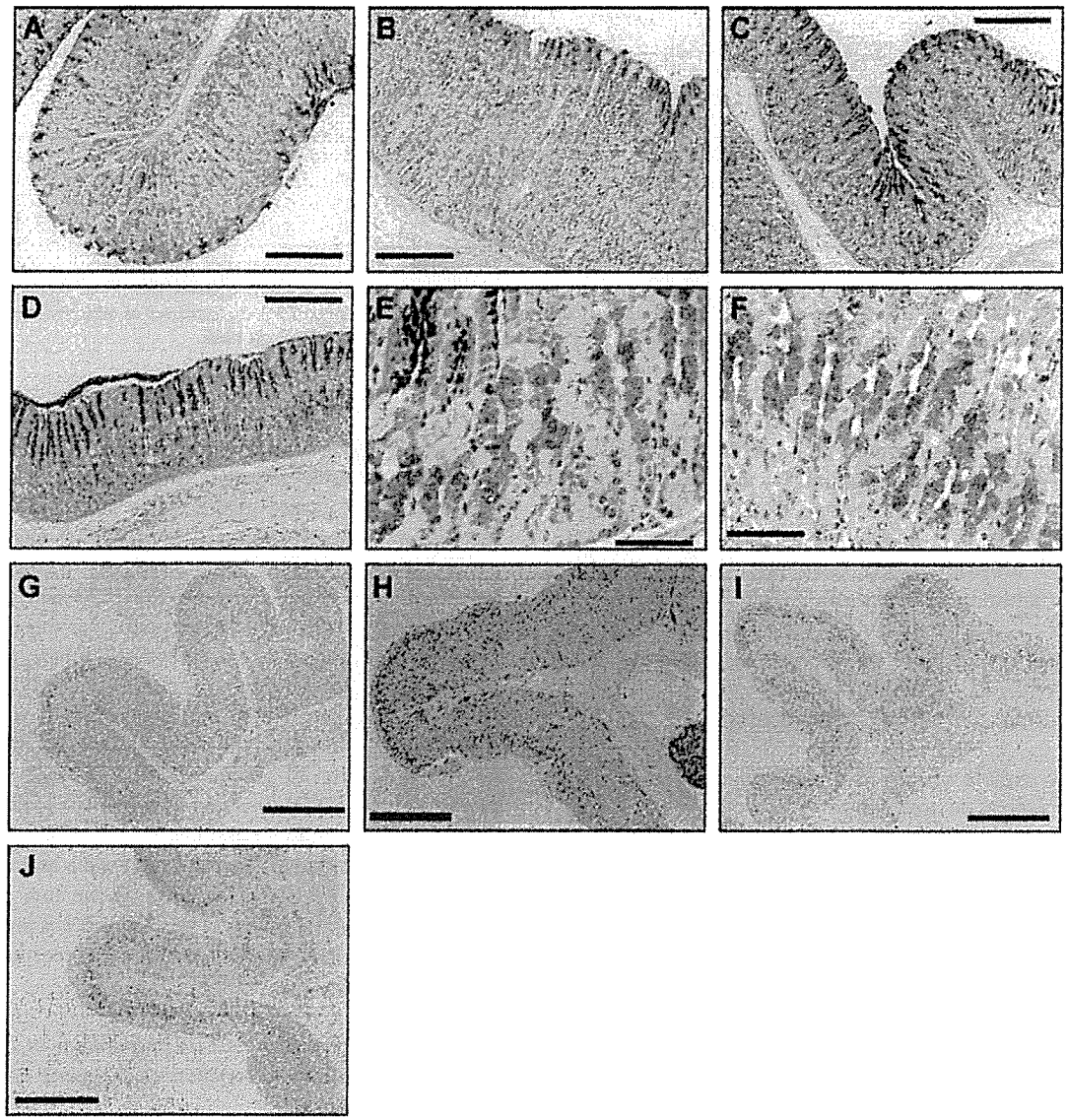


Fig. 3. Oxyntic mucosa from 10-week-old wild-type, histamine $H_2$ receptor-null, gastrin receptor-null and double-null mice. Sections of oxyntic mucosa from wild-type (A, G), histamine $H_2$ receptor-null (B, H), gastrin receptor-null (C, E, I) and double-null (D, F, J) mice were subjected to PAS staining (A, B, C, D, E, F) or BrdU labeling (G, H, I, J). Scale bars, 200 μm (A, B, C, D), 50 μm (E, F), 500 μm (G, H, I, J).

arbitrary units per gland vs. 20.3±0.5 arbitrary units per gland, $P<0.001$) (Table 1, Fig. 3C). Thus, although numbers of downward migrating cells were decreased, the total number of cells per gland did not differ significantly between gastrin receptor-null and wild-type mice (Table 1). In addition, an increase in the number of BrdU positive cells per gland was observed in gastrin receptor-null mice (gastrin receptor-null, 2.76±0.14 arbitrary units per gland, wild-type, 0.95±0.09 arbitrary units per gland, $P<0.001$) (Table 1, Fig. 3I). Just as in histamine $H_2$ receptor-null mice, some portions of the oxyntic mucosa, especially at the greater curvature and near the antrum, contained mucous neck cells full of mucins (Fig. 3E). Small parietal cells were observed in gastrin receptor-null mice as well (gastrin receptor-null mice, 5.37±0.10 arbitrary units per cell, wild-type mice, 8.86±0.17 arbitrary units per cell, $P<0.001$) (Table 1). In double-null mice, numbers of ECL cells, and parietal cells as well as the total number of downward migrating cells, were decreased (Table 1). As in gastrin receptor-null mice, the number of surface mucous cells was increased as compared with those from wild-type mice (25.3±0.8 arbitrary units per gland vs. 20.3±0.5 arbitrary units per gland, $P<0.001$) (Table 1, Fig. 3D). BrdU positive cells per gland were increased in number in double-null mice (double-null, 1.75±0.13 arbitrary units per gland, wild-type, 0.95±0.09 arbitrary units per gland, $P<0.001$) (Table 1, Fig. 3J). Total number of cells per gland did not differ significantly between wild-type and double-null mice (Table 1). Mucous neck cells with

Table 1
Quantitative analyses of gastric glands from 10-week-old wild-type, histamine $H_2$ receptor-null, gastrin receptor-null and double-null mice

| | Total cell number | Surface mucous cell number | Gland cell number | Parietal cell | | ECL cell number | BrdU positive cell number |
|---|---|---|---|---|---|---|---|
| | | | | Number | Size | | |
| Wild-type | 63.7±0.7 | 20.3±0.5 | 43.4±0.7 | 20.3±0.4 | 8.86±0.17 | 1.44±0.13 | 0.95±0.09 |
| Histamine $H_2$ receptor-null | 114.2±3.6[a] | 26.7±1.6[a] | 87.5±2.9[a] | 38.6±1.3[a] | 4.79±0.11[a] | 7.61±0.32[a] | 2.01±0.11[a] |
| Gastrin receptor-null | 61.5±1.2 | 26.7±0.7[a] | 34.8±0.9[a] | 13.8±0.2[a] | 5.37±0.10[a] | 0.53±0.08[a] | 2.76±0.14[a] |
| Double-null | 61.1±1.1 | 25.3±0.8[a] | 35.8±0.8[a] | 14.2±0.4[a] | 5.01±0.09[a] | 0.81± 0.07[a] | 1.75±0.13[a] |

Numbers of cells were counted in gastric glands sectioned centrally and in a manner parallel to their longitudinal axes, then expressed as arbitrary units per gland. Parietal cell size was determined by measuring the longitudinal cross sectional area of parietal cells from these gastric glands and expressed as arbitrary units per cell. One hundred glands from 10 mice (10 glands per mouse) were used for each type of mouse. Data are expressed as arbitrary units per gland or parietal cell since the data obtained are proportional but not equivalent to the actual cell numbers or parietal cell mass.

[a] $P<0.0001$ vs. wild-type mice.

characteristics similar to those in histamine $H_2$ receptor-null mice and gastrin receptor-null mice were seen in similar portions of the gastric mucosa (Fig. 3F). Small parietal cells were also observed in double-null mice (double-null mice, 5.01±0.09 arbitrary units per cell, wild-type mice, 8.86±0.17 arbitrary units per cell, $P<0.001$) (Table 1).

### *3.2. Comparison of chief cell lineage in gastric mucosae from 10-week-old wild-type, histamine $H_2$ receptor-null, gastrin receptor-null and double-null mice*

Next, to explore the effects of histamine $H_2$ receptor and gastrin receptors on maturation of the chief cell lineage, expressions of pepsinogen and type III mucin were examined in gastric glands in each type of mouse. Fig. 4 is a schematic representation of a gastric gland. Fig. 5 shows that type III mucin positive cells were increased in number in histamine $H_2$ receptor-null, gastrin receptor-null and double-null mice as compared with wild-type mice. In addition, type III mucin positive cells, although present in the base regions of gastric glands from histamine $H_2$ receptor and double-null mice (Fig. 5J,L), were very scarce at the bases of gastric glands from wild-type and gastrin receptor-null mice (Fig. 5I,K). In wild-type mice, numbers of pepsinogen positive cells in gastric glands gradually increased from the isthmus to the base and pepsinogen expression per cell had already peaked in the neck region (Fig. 5A). In gastrin receptor-null mice, pepsinogen expression in gastric glands was maximal only at the base (Fig. 5C). It is noteworthy that mature chief cells, without type III mucin and with abundant pepsinogen, were present at the base region of gastric glands from gastrin receptor-null mice (Fig. 5C,G). In contrast, gland cells with abundant pepsinogen expression and without type III mucin were not present in histamine $H_2$ receptor-null mice and double-null mice (Fig. 5B,D,F,H). In addition to the low pepsinogen expression, pepsinogen levels per cell did not increase from the isthmus to the base in histamine $H_2$ receptor-null and double-null mice (Fig. 5B,D).

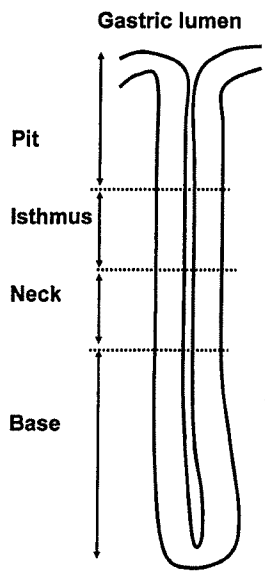


Fig. 4. Schematic drawing of a gastric gland.

### *3.3. Gastric pH and gastric acid productions in 10-week-old wild-type, histamine $H_2$ receptor-null, gastrin receptor-null and double-null mice*

First, in vivo acid productions in response to secretagogues were measured. Histamine $H_2$ receptor-null mice were responsive to carbachol, but not to histamine or gastrin-17 (Fukushima et al., 2003). Secretagogue-induced acid secretion (10 mg/kg BW of histamine, 0.05 mg/kg BW of carbachol) was not observed in either gastrin receptor-null nor double-null mice (data not shown). Gastric pH values in double-null mice were the highest among the four types of mice (Fig. 6). Those in gastrin receptor-null mice were higher than those in wild-type or histamine $H_2$ receptor-null mice and lower than those in double-null mice. Treatment of gastrin receptor-null mice with famotidine (10 mg/kg BW) or pirenzepine (10 mg/kg BW) raised gastric pH values, indicating that histaminergic and muscarine pathways, although severely impaired, are functional in gastrin receptor-null mice. Because fasting gastric pH values in double-null mice were too high to assess the inhibitory effects of pirenzepine, the effect of

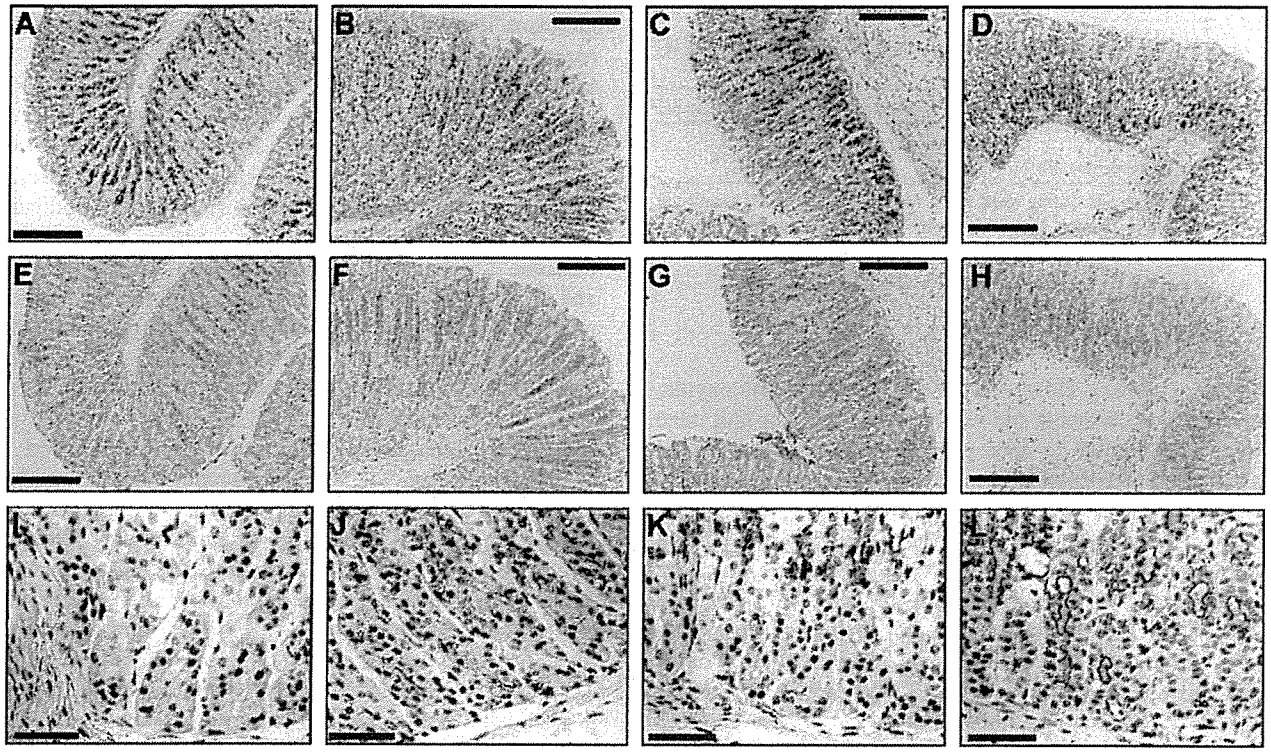


Fig. 5. Expressions of pepsinogen and type III mucin in oxyntic mucosa from 10-week-old wild-type, histamine $H_2$ receptor-null, gastrin receptor-null and double-null mice. Sections of oxyntic mucosa from wild-type (A, E, I), histamine $H_2$ receptor-null (B, F, J), gastrin receptor-null (C, G, K) and double-null (D, H, L) mice were stained with anti-pepsinogen antibody (A, B, C, D) and anti-type III mucin antibody (E, F, G, H, I, J, K, L). In I, J, K, L, type III mucin-positive cells are marked with asterisks. Scale bars, 200 μm (A, B, C, D, E, F, G, H), 50 μm (I, J, K, L).

carbachol at 1 mg/kg BW, a dose which is too high to be tolerated in measuring in vivo acid production, was examined in double-null mice. Fig. 6 shows that while gastrin receptor-null mice were responsive to both histamine and carbachol, double-null mice were unresponsive to both.

### *3.4. Long term follow-up of histamine $H_2$ receptor-null mice and double-null mice*

At 6 months, while there were no changes in gastric mucosa from wild-type mice, further elongation of gastric glands was observed in histamine $H_2$ receptor-null mice

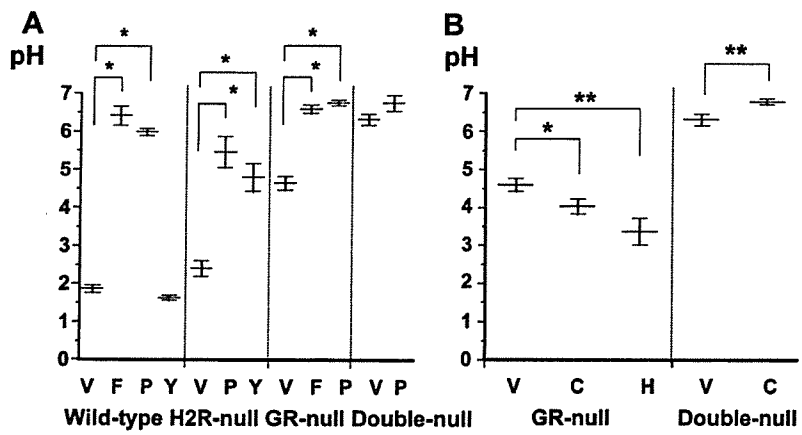


Fig. 6. Gastric pH in wild-type, histamine H2 receptor-null, gastrin receptor-null and double-null mice. Wild-type, histamine $H_2$ receptor-null (H2R-null), gastrin receptor-null (GR-null) and double-null (10 to 12 weeks old) mice were fasted overnight with free access to water. (A) At 1.5 h after subcutaneous injection of 0.5% methylcellulose as a vehicle (V) ($n$=20), 10 mg/kg BW of famotidine (F) ($n$=20), 10 mg/kg BW of pirenzepine (P) ($n$=20) or 10 mg/kg BW of YM022 (Y) ($n$=20), the mice were killed and their stomachs immediately excised. Gastric pH was measured using an ultra-thin pH monitor. (B) At 15 min after subcutaneous injection of vehicle (V) ($n$=20), 10 mg/kg BW of histamine (H) ($n$=20) or 1 mg/kg BW of carbachol (C) ($n$=20), the mice were killed and their stomachs immediately excised. Gastric pH was measured using an ultra-thin pH monitor. Data are presented as means±S.E. *$P$<0.001 vs. respective values.

Table 2
Stomach weight and gastric pH in aged wild-type and aged histamine $H_2$ receptor-null mice

| | Stomach weight (g) | Fasting gastric pH |
|---|---|---|
| Wild-type | 0.16±0.02 | 1.61±0.13 |
| Histamine $H_2$ receptor-null | 0.38±0.02[a] | 2.14±0.13[b] |

Stomach weight and fasting gastric pH were measured in 12-month-old wild-type and histamine $H_2$ receptor-null mice. Data are expressed as means±S.E. ($n$=10, each group).
[a] $P$<0.0001 vs. wild-type mice.
[b] $P$=0.0134 vs. wild-type mice.

(data not shown). However, the structure of gastric oxyntic mucosa from 6-month-old histamine $H_2$ receptor-null mice was very similar to that of mucosa from 10-week-old histamine $H_2$ receptor-null mice, except for the presence of cysts near the basal region. In 12-month-old histamine $H_2$ receptor-null mice, in addition to the marked increase in stomach weight (Table 2), oxyntic mucosal structures appeared to differ strikingly from those of wild-type and younger histamine $H_2$ receptor-null mice (Fig. 7B). Oxyntic mucosa from aged histamine $H_2$ receptor-null mice was full of cystic structures (Fig. 7B). Most gastric glands were dilated and, in addition, interstitial tissues between cysts were markedly increased (Fig. 7D), which is in sharp contrast to the findings in gastric mucosa from aged wild-type mice (Fig. 7C). Some cells lining the cysts were positive for $H^{(+)}/K^{(+)}$-ATPase, pepsinogen and HDC (Fig. 7E,F,G), indicating that the cysts were derived from dilated gastric glands. However, small portions of oxyntic mucosa remained mostly unaltered (Fig. 7H), suggesting that the program for formation of normal gastric glands is preserved in gastric mucosal stem cells. Gastric pH values in aged histamine $H_2$ receptor-null mice were essentially preserved (Table 2). Similar features were observed in gastric mucosae from 24-month-old histamine $H_2$ receptor-null mice (data not shown). Unlike histamine $H_2$ receptor-null mice, there were no significant differences in oxyntic mucosae between 10-week-old and 12-month-old double null mice (data not shown).

## 4. Discussion

Oxyntic mucosal atrophy in double-null mice confirms the oxyntic mucosal hypertrophy observed in histamine $H_2$ receptor-null mice to be due to stimuli delivered via gastrin receptors. In double-null and gastrin receptor-null mice, numbers of gland cells as a whole (downward migrating cells) were decreased. However, despite gastric mucosal atrophy surface mucous cell number was moderately but significantly increased in gastrin receptor-null and double-null mice as compared with wild-type mice (Table 1). Turnover of surface mucous cells is far faster than that of downward migrating cells (Karam and Leblond, 1992, 1993a,b,c,d, 1995). Thus, it is likely that most of the increases in BrdU labeling in oxyntic mucosae in gastrin receptor-null and double-null mice are attributable to increased growth and differentiation into surface mucous cells. In the case of gastrin-null mice, the percentage of BrdU positive cells in oxyntic mucosa was not different from that in wild-type mice and there was a marked decrease in the surface mucous cells in gastrin-null mice as compared with wild-type mice (Koh et al., 1997). Thus, gastric mucosae from gastrin receptor-null and double-null mice and those from gastrin-null mice are different in terms of number of surface mucous cells. Post-translational modification of preprogastrin yields progastrin and glycine-extended gastrin as well as gastrin-17 (Dockray et al., 2001). In G-cells, gastric mucosal processing of preprogastrin yields gastrin and glycine-extended gastrin (Dockray et al., 2001). Glycine-extended gastrin reportedly has very low affinity for the gastrin receptor and has been suggested to interact with a novel receptor, which remains to be identified (Dockray et al., 2001). Thus, serum and oxyntic mucosal levels of glycine-extended gastrin may well be elevated, like those of gastrin-17, in gastrin receptor-null and double-null mice. In a study using gastrin-null mice, infusion of gastrin-17 and glycine-extended gastrin had distinct effects on gastric acid secretion, via different signal transduction pathways (Chen et al., 2000; Hollande et al., 2001; Stepan et al., 1999). Thus, the absence of glycine-extended gastrin effects in gastrin-null mice and possible hyperstimulation of the glycine-extended gastrin receptor in gastrin receptor-null mice might account for the difference in surface mucus cells in these mice. The finding of similar surface mucous cell increases in double-null mice indicates that a glycine-extended gastrin-dependent increase in surface mucous cells in the absence of gastrin receptors is not dependent on the histamine $H_2$ receptor. We speculate that a similar increase in surface mucous cell number in histamine $H_2$ receptor-null mice was caused by such a glycine-extended gastrin effect. Taken together, our results show gastrin and glycine extended-gastrin to have distinct roles in the growth of gastric mucosa.

We previously reported that maturation of the chief cell lineage was impaired in gastric mucosa from histamine $H_2$ receptor-null mice (Fukushima et al., 2003). In this report, mature chief cells, which we define as being positive for pepsinogen and negative for type III mucin, were present gastrin receptor-null mouse. In contrast, in histamine $H_2$ receptor-null mice and double-null mice expression levels of pepsinogen per cell are very low and mature chief cells were very scarce. Considering the marked difference in pH values in histamine $H_2$ receptor-null mice and double-null mice (Fig. 6), the difference in chief cells in these mice is not attributable to low acidity but rather to disruption of the histamine $H_2$ receptor itself. Genetic ablation of parietal cells with $H^{(+)}/K^{(+)}$-ATPase promoter resulted in loss of mature chief cells, which can be taken as evidence that parietal cells are involved in chief cell maturation (Canfield et al., 1996; Li et al., 1996). However, it has been suggested